OCEAN DRILLING PROGRAM
LEG 175 PRELIMINARY REPORT

BENGUELA CURRENT

Dr. Wolfgang Berger
Co-Chief Scientist, Leg 175
Mail Code A-015
SIO-Geological Research Division
University of California at San Diego
La Jolla, California 92093-0215
U.S.A.

Dr. Gerold Wefer
Co-Chief Scientist, Leg 175
Fachbereich Geowissenschaften
Universität Bremen
Postfach 330440
D-28334 Bremen
Germany

Dr. Carl Richter
Staff Scientist, Leg 175
Ocean Drilling Program
Texas A&M University Research Park
1000 Discovery Drive
College Station, Texas 77845-9547
U.S.A.

Paul J. Fox
Director
of Science Operations
ODP/TAMU

Thomas A. Davies
Manager
Science Services
ODP/TAMU

Jack Baldauf
Deputy Director
of Science Operations
ODP/TAMU

January 1998

This informal report was prepared from the shipboard files by the scientists who participated in the cruise. The report was assembled under time constraints and is not considered to be a formal publication which incorporates final works or conclusions of the participating scientists. The material contained herein is privileged proprietary information and cannot be used for publication or quotation.

Preliminary Report No. 75

First Printing 1998

Distribution

Electronic copies of this publication may be obtained from the ODP Publications Home Page on the World Wide Web at: http://www-odp.tamu.edu/publications

D I S C L A I M E R

This publication was prepared by the Ocean Drilling Program, Texas A&M University, as an account of work performed under the international Ocean Drilling Program, which is managed by Joint Oceanographic Institutions, Inc., under contract with the National Science Foundation. Funding for the program is provided by the following agencies:

Australia/Canada/Chinese Taipei/Korea Consortium for Ocean Drilling
Deutsche Forschungsgemeinschaft (Federal Republic of Germany)
Institut Français de Recherche pour l'Exploitation de la Mer (France)
Ocean Research Institute of the University of Tokyo (Japan)
National Science Foundation (United States)
Natural Environment Research Council (United Kingdom)
European Science Foundation Consortium for the Ocean Drilling Program (Belgium, Denmark, Finland, Iceland, Italy, The Netherlands, Norway, Portugal, Spain, Sweden, Switzerland, and Turkey)

Technical Editor: Karen K. Graber

SCIENTIFIC REPORT

The following scientists were aboard the *JOIDES Resolution* for Leg 175 of the Ocean Drilling Program:

Wolfgang Berger, Co-Chief Scientist (Scripps Institution of Oceanography, University of California at San Diego, Geosciences Research Division, La Jolla, California 92093, U.S.A. E-Mail: wberger@ucsd.edu)

Gerold Wefer, Co-Chief Scientist (Faculty of Earth Sciences (FB 5), University of Bremen, Postfach 330440, 28334 Bremen, Germany. E-Mail: gwefer@allgeo.uni-bremen.de)

Carl Richter, Staff Scientist (Ocean Drilling Program, Texas A&M University Research Park, 1000 Discovery Drive, College Station, Texas 77845. E-Mail: Richter@tamu.edu)

Donald D. Adams, Organic Geochemist (Center for Earth and Environmental Science, State University of New York, Plattsburgh, New York 12901, U.S.A. E-Mail: adamsdd@splava.cc.plattsburgh.edu)

Linda Davis Anderson, Sedimentologist (Institute of Marine Sciences, University of California at Santa Cruz, Santa Cruz, California 95064, U.S.A. E-Mail: linda@cats.ucsc.edu)

Dyke J. Andreasen, Physical Properties Specialist (Earth Sciences Board, University of California at Santa Cruz, Santa Cruz, California 95064, U.S.A. E-Mail: andreasn@cats.ucsc.edu)

Volker Brüchert, Sedimentologist (Department of Geological Studies, Biochemical Laboratories, Indiana University, Bloomington, Indiana 47405, U.S.A. E-Mail: vbrucher@indiana.edu)

Hervé Cambray, LDEO Logging Specialist (Cerege, Domaine de L'Arbois, 13545 Aix-en-Provence, France. E-Mail: cambray@arbois.cerege.fr)

Beth A. Christensen, Paleontologist (Department of Geological Sciences, University of South Carolina, Columbia, South Carolina 29208, U.S.A. E-Mail: bac@geol.sc.edu)

Gina M. Frost, Paleomagnetist (Earth Sciences Board, University of California at Santa Cruz, Santa Cruz, California 95064, U.S.A. E-Mail: gfrost@earthsci.ucsc.edu)

Jacques Giradeau, Paleontologist (Département de Géologie et Océanographie, Université de Bordeaux 1, Avenue des Facultés, Talence Cedex 33405, France. E-Mail: giraudeau@geocean.u-bordeaux.fr)

Thomas J. Gorgas, Physical Properties Specialist (University of Hawaii, Manoa, 2525 Correa Rd., Honolulu, Hawaii 96822, U.S.A. E-Mail: tgorgas@soest. hawaii.edu)

Otto Hermelin, Paleontologist (Deep Sea Geology Division, University of Stockholm, S-106 91 Stockholm, Sweden. E-Mail: otto.hermelin@geol.su.se)

J.H.Fred Jansen, Sedimentologist (Netherlands Institute for Sea Research, P.O. Box 59, 1790 AB Texel, The Netherlands. E-Mail: jansen@nioz.nl)

Carina Beatriz Lange, Paleontologist (Scripps Institution of Oceanography, University of California at San Diego, 9500 Gilman Drive, GRD-0215, La Jolla, California 92093-0215, U.S.A. E-Mail: clange@ucsd.edu

Bernd Laser, Physical Properties Specialist (Department of Earth Sciences , University of Bremen, FB 5, Postfach 330440, 28334 Bremen, Germany. E-Mail: bela@uni-bremen.de)

Hui-Ling Lin, Sedimentologist (Institute of Marine Geology and Chemistry, National Sun Yat-Sen Universitiy, Kaohsiung 804 Taiwan. E-Mail: hllin@mail.nsysu.edu.tw)

Mark Maslin, Sedimentologist (Environmental Change Research Center, Department of Geography, University College London, 26 Bedford Way, London WC1H 0AP, United Kingdom. E-Mail: mmaslin@geog.ucl.ac.uk)

Philip A. Meyers, Inorganic Geochemist (Department of Geological Sciences, University of Michigan, 2534 C.C. Little Building, 425 East University Avenue, Ann Arbor, Michigan 48109-1063, U.S.A. E-Mail: pameyers@umich.edu)

Isao Motoyama, Paleontologist (Department of Physics and Earth Sciences, University of the Ryukyus, Senbaru 1, Nishihara-cho, Okinawa 903-01, Japan. E-Mail: motoyama@sci.u-ryukyu.ac.jp)

Richard W. Murray, Inorganic Geochemist (Department of Earth Sciences, Boston University, 675 Commonwealth Avenue, Boston, Massachusetts 02215, U.S.A. E-Mail: rickm@bu.edu)

David Pato, Angolan Observer (Ministério de Geologia E Minas, Luanda, Republica de Angola. E-Mail: None)

Maria Elena Perez, Sedimentologist (Geosciences Research Division, Scripps Institution of Oceanography, University of California at San Diego, 9500 Gilman Drive, La Jolla, California 92093-0215, U.S.A. E-Mail: meperez@ucsd.edu)

Peir Kenneth Pufahl, Sedimentologist (Department of Earth and Ocean Sciences, University of British Columbia, 6339 Stores Road, Vancouver, BC V6T 1Z4, Canada E-Mail: ppufahl@eos.ubc.ca)

Volkhard Spiess, Physical Properties Specialist (Department of Earth Science, University of Bremen, Postfach 330440., 28334 Bremen, Germany. E-Mail: a13g@zfn.uni-bremen.de)

Laurence Vidal, Sedimentologist (Geosciences, University of Bremen, Postfach 330440, 28334 Bremen, Germany. E-Mail: vidal@uni-bremen.de)

Rochelle Wigley, South African Participant/Inorganic Geochemist (Werner Marine Research (PTY) LTD, University of Cape Town, 836 Sanlam Business Park, Koeberg Road, Milnerton,7441, Cape Town, South Africa. E-Mail: c/o compton@geology.vct.ac.sa)

Toshitsugu Yamazaki, Paleomagnetist (Marine Geology Department, Geological Survey of Japan, 1-1-3 Higashi, Tsukuba, Ibaraki 305, Japan. E-Mail: yamazaki@gsj.go.jp)

ABSTRACT

During Leg 175, thirteen sites were occupied off the western coast of Africa (Congo, Angola, Namibia, and South Africa), and 40 holes were drilled using advanced hydraulic piston coring and the extended core barrel method. The goal is to reconstruct the late Neogene history of the Benguela Current and the associated upwelling regimes between 5° and 32°S. The area investigated contains one of the greatest upwelling regions of the world, intermediate in intensity between the systems off Peru and California. The Angola-Benguela Current system with its associated upwelling regions ("ABC-system") is characterized by organic-rich sediments that contain an outstanding record of productivity history, which can be read on a very fine scale. In addition, this environment provides an excellent setting for natural experiments in diagenesis.

The individual transects selected for drilling within the ABC-system reflect a compromise among geographic coverage, accessibility, quality of sedimentary record, and time constraints. Variations in productivity are generated in different ways, within different geographic settings (off the Congo, near the Angola Dome, at Walvis Ridge, in the upwelling cells south of the ridge). One of the major goals is to document fluctuations in productivity in these different settings in relationship to large-scale climate change within the late Neogene, including the onset of glacial cycles in the Northern Hemisphere. Another major goal is to tie the fluctuations in oceanic conditions to the corresponding changes in climate on the adjacent continent.

Most of the sites drilled have high sedimentation rates (ca. 100 m/m.y.), which offers an opportunity to develop detailed paleoceanographic records, with a resolution near 1000 yr. Sediments are largely diatomaceous and carbonate-rich clays with variable (and occasionally very high) organic carbon contents. Analysis of these sediments will greatly extend and refine results concerning paleoceanography and paleoclimate of the late Neogene that were provided by Deep Sea Drilling Project Sites 362 and 532.

The northernmost sites (Sites 1075, 1076, and 1077) contain the record of sediment supply by the Congo River, intercalated with the oceanic record. Pollen, freshwater diatoms, phytoliths, and clay

minerals will provide clues to climatic change in the drainage basin of the Congo. Fluctuations in the accumulation of pelagic diatoms and of marine organic matter track the changes in productivity in this peri-estuarine environment.

Sedimentation patterns at Sites 1078 and 1079 are greatly influenced by changes in intensity of upwelling around the Angola Dome. The two sites show extremely high rates of accumulation, presumably due to the supply of silt from vigorous coastal erosion (as seen in the morphology of the coast around Lobito). Sediments of Site 1081 contain a record of variation in seasonal coastal upwelling near the northern boundary of the string of coastal upwelling cells off Namibia and South Africa ("southwest Africa upwelling cells"). This record is closely related to the southeasterly winds driving the Benguela Current, which is documented (in part) in the supply of dust from the Namib Desert. Sites 1082, 1083, and especially 1084, lie close to the major upwelling centers along southwest Africa, with year-round upwelling activity. Thus, these sites directly record the variability in the intensity of coastal upwelling, mainly through the eddies and filaments generated at the centers and passing overhead and generating high export production. The three sites in the southern part of the Cape Basin (1085, 1086, and 1087) document the history of the Benguela Current near its point of origin and contain a record of the influence of warm water from the Indian Ocean, brought by the Agulhas Current. Also, these sites contain the evidence for incursions of cold antarctic waters, which apparently reached a maximum near the Pliocene/Pleistocene boundary.

Preliminary results focus on the interplay between high- and low-latitude Milankovitch forcing (obliquity vs. precession), the role of the 100-k.y. oscillation, the effects of the mid-Pleistocene Climate Step (near 920 ka) on upwelling and African climate, the nature of the late Pliocene-early Pleistocene productivity maximum, the onset of enhanced upwelling at the beginning of the late Pliocene (near 3 Ma), and the implications of changes in productivity and sediment supply for diagenesis, which affects interpretation of seismic profiles. Concerning this latter item, dolomite layers were found to be abundant at certain sites, whereas evidence for clathrates was lacking at all sites.

INTRODUCTION

The ocean's role in climatic change through heat transport and control of carbon dioxide is increasingly being recognized. This new awareness, and the urgency that must be accorded the attempt to understand the mechanisms of climatic change, have led to the initiation of large integrated efforts in physical and chemical oceanography. Likewise, the potential of the oceanic record for understanding climatic change has received increased attention in recent years (CLIMAP, 1976; COSOD II, 1987). The Angola/Namibia high-productivity system needs to be studied because of its importance in the global ocean-carbon cycle and to provide for comparison with the Peru and California systems. Only by comparing these systems with each other shall we be able to learn which elements of a system are peculiar, and which have general validity through time and on a global scale. To further these goals, 13 advanced hydraulic piston corer and extended core barrel (APC/XCB) sites were drilled off the southwestern coast of Africa during Leg 175 (Fig. 1) to study the paleoenvironment of the Benguela Current and Angola/Namibia upwelling system, with emphasis on the late Neogene.

Eastern boundary upwelling is strongly involved in modulation of the carbon cycle and, therefore, in control of the partial pressure of carbon dioxide (pCO_2) ("biological pumping"; Berger and Keir, 1984; Sundquist and Broecker, 1985; Boyle and Keigwin, 1987; Sarnthein et al., 1988; Berger et al., 1989). It is now generally thought that such pumping is a crucial factor for the explanation of the type of short-term fluctuations in atmospheric CO_2 seen in ice cores (Barnola et al., 1987). Along these lines of argument, there is a good correlation between productivity indices in the eastern equatorial Pacific and the ice-core record of pCO_2. Likewise, there is good correlation between the ice-core record and estimates of CO_2 pressure in surface water.

On a longer time scale, Vincent and Berger (1985) have postulated that depositional pumping by coastal upwelling is responsible for changing the general level of atmospheric pCO_2. They propose a climatic preconditioning by upwelling-induced carbon extraction from the ocean-atmosphere

system for the beginning of the modern ice-cap dominated world. Their argument is based on the observation that carbon isotopes in deep-sea benthics become ^{13}C enriched just when organic-rich phosphatic sediments begin to accumulate around the Pacific margins. In this view, eastern boundary upwelling, and therefore upwelling off Angola and Namibia, has global implications for the long-term history of the carbon cycle and climate and for the evolution of life and biogeography on land and in the sea.

To be able to predict the effects of changes in productivity on the CO_2 content of the atmosphere, the interrelationships among ocean circulation, nutrient transport, and the sedimentation of organic compounds and carbonate must be established for each of the important productivity regions. Until now, there has been no information on Neogene upwelling fluctuations off Angola and Namibia, a region that is probably of considerable importance for the global carbon cycle.

The most important period for understanding the workings of the present system is the time since the Miocene. Within this period, we see the evolution of the present planetary orography, the buildup of ice caps on both poles, the development of modern wind and upwelling regimes, and the stepwise increase in North Atlantic Deep Water (NADW) production, which dominates the style of deep circulation in the ocean. The present system is characterized by a strong 100,000-yr climatic cycle, beginning 700,000 yr ago (Berger et al., 1996). High-amplitude fluctuations associated with buildup and decay of northern ice sheets began around 2.8 m.y. ago (Shackleton et al., 1984; Hodell and Venz, 1992).

BACKGROUND

The Angola/Namibia system is one of five or six great upwelling regions in the world. It extends over a considerable portion of the western margin of South Africa, with productivity values ≥ 180 g˚C/m^{2}yr. It is characterized by organic-rich sediments containing an excellent record of productivity history, which, in turn, is closely tied to the regional dynamics of circulation, mixing, and upwelling, as seen in the oxygenation of thermocline waters. In addition, this environment

provides an excellent setting for "natural experiments" in diagenesis, especially concerning the genesis of economically important resources (e.g., petroleum and phosphate).

Upwelling off southwest Africa is at present centered on the inner shelf and at the shelf edge. The Benguela Current flows roughly parallel to the coast and within ~180 km of it south of 25˚S, and then turns to the west over the Walvis Ridge between 23˚ and 20˚S. At about 20˚S, warm, tropical water masses from the north meet the cold Benguela Current water. Eddies of cold, upwelled water contain radiolarian and diatom skeletons, which are transported from the upwelling area to the northern part of the Walvis Ridge, where they have been sampled at Deep Sea Drilling Project (DSDP) Sites 532 (Hay, Sibuet, et al., 1984) and 362 (Bolli, Ryan, et al., 1978).

According to previous studies, during the last glacial maximum (LGM) eddies formed farther north, and the Benguela Current flowed parallel to the coast and over the Walvis Ridge to reach the Angola Basin, finally bearing to the west at about 17˚S. Sediments deposited at Site 532 during the LGM apparently confirm the absence of upwelling eddies by containing zero to very few opal skeletons (Hay, Sibuet, et al., 1984; Diester-Haass, 1985). Upwelling may have continued to occur on the African shelf, but the Benguela Current did not transport that upwelling signal to the Walvis Ridge. However, from the distribution of foraminifer assemblages at Site 532, it appears that the northeastern Walvis Ridge was in fact characterized by intensified upwelling and a westward expansion of coastal upwelling cells at glacial periods during the last 500,000 yr (Oberhänsli, 1991). The issue of contrasting models of glacial/interglacial upwelling dynamics in this region is unresolved. It hinges on the question of why opaline fossils show contrary abundance variations with respect to the productivity record from other proxy indicators.

The results from Sites 362 and 532 can be used tentatively to reconstruct the evolution of the Benguela Current during the past 10 m.y. This evolution is characterized, on the whole, by increasing rates of accumulation of organic carbon. In addition, there are indications from changing correlations between percent carbonate, percent C_{org}, and diatom abundance that the dynamics of the system undergo stepwise modifications. In this connection, as well, a distinct opal maximum in the early Quaternary is of great interest. The nature of this transition is not clear; perhaps it is a

response to the migration of the polar front to its modern position.

The evolution of the climate of the Northern Hemisphere, and particularly that of northern Europe, is linked to the exchange of heat between the South Atlantic and the North Atlantic Oceans. This energy transport, operating over large distances, is involved in the formation and magnitude of polar ice caps. In today's world, a net heat transfer from the South Atlantic to the North Atlantic exists in currents above the thermocline. A part of the heat contribution from the South Atlantic is believed to originate from the Indian Ocean via the Agulhas Current. The Benguela Current is a connection between the waters north of the polar front in the South Atlantic and the Equatorial Currents of the Atlantic. Northward and southward shifts of the Southern Ocean polar front constrict or expand, respectively, the interchange of heat from the Indian Ocean to the South Atlantic (McIntyre et al., 1989). This interchange presumably has a drastic impact on the heat budget of the Benguela Current and, consequently, that of the entire Atlantic Ocean. Such variations in heat transfers should appear as changes in the course and intensity of currents and productivity regimes and should be recorded in the sediments accumulating along the southwest African margin.

An important element of the heat transfer dynamics is the deep-circulation pattern. Traditionally, the focus in reconstructing this pattern has been on the properties and boundaries of NADW-related water masses, as seen in the $\delta^{13}C$ of benthic foraminifers. The emphasis has been on glacial-to-interglacial contrast. This contrast shows that NADW production was greatly reduced during glacial periods (also reflected in the pattern of carbonate preservation). More recent studies have added much detail to this story (summarized in Bickert and Wefer, 1996). It appears that the strength of the NADW is reflected in the differences between eastern and western basins and in gradients within the eastern basin. Information on associated changes at depths above the NADW has been sparse. It must be assumed that the strength of the nutrient maximum underlying the Benguela upwelling regions is somehow coupled to the evolution of NADW, which in turn influences the dynamics of intermediate water-mass formation to the south. At this point, we do not know how the different cycles are related, so little or nothing can be said about causal relationships.

Paleoceanographic interpretations regarding the history of the Benguela Current are derived mainly from a single location off southwest Africa (Site 532) and must be considered preliminary. Given the indications that the axis and the intensity of the Benguela Current have changed over the past 15 m.y. and that productivity has fluctuated with glacial/interglacial cycles, confirmation and refinement of these ideas is needed. Although sites in the Cape and Angola Basins and on the Walvis Ridge were occupied during DSDP Legs 40, 74, and 75, these sites are situated too far offshore to provide the needed information. The Benguela Current and its associated upwelling regions are not recorded well in the sediments at these sites. Even Sites 362 and 532 on the Walvis Ridge are too far offshore to contain a direct record of upwelling activity. They receive an indirect record of near-coastal upwelling from material transported to their location by the Benguela Current. Furthermore, modern coring technology (APC and XCB) allows for high-resolution studies by avoiding much of the drilling disturbance present in the Leg 40 cores. Such high-resolution work is crucial if the dynamics of upwelling are to be captured back to the Miocene on a scale of glacial/interglacial cycles. Information from an array of sites situated in the Southern and Mid-Cape Basins, on the Walvis Ridge, and in the southern Angola Basin would allow the construction of a coherent picture.

SCIENTIFIC OBJECTIVES

The results from DSDP Sites 362 and 532 suggest that there has been a general northward migration of the Benguela Current upwelling system during the last 14 m.y. Because the shape of the South Atlantic has not changed appreciably during this time, the changes in the upwelling system must reflect large-scale, perhaps global, changes in ocean circulation. Leg 175 will focus primarily on the paleoceanographic and paleoclimatic aspects of the area. However, there is interest in investigating samples from the upwelling area off Angola and Namibia with regard to early diagenetic processes taking place in this unique environment. Possible work includes study of the formation of dolomite (Baker and Kastner, 1981; Kulm et al., 1984), phosphorite (Calvert and Price, 1983), and chert (see articles in Garrison et al., 1984). We will also be able to examine the organic matter type and distribution as a function of time and climatic cycles. Important questions

that are being addressed by Leg 175 include the following:

- Determine the history of the Benguela Current for the late Neogene. Of special interest is the changing response to orbital forcing, as seen in spectral amplitudes and phase relationships (e.g., McIntyre et al., 1989; Schneider, 1991; Berger and Wefer, 1996; Jansen et al., 1996; Schneider et al., 1996; Wefer et al., 1996).

- Study the history of productivity of the upwelling region off Angola and Namibia and the influence of the Zaire River, extending available information about the late Quaternary (Bremner, 1983; Jansen et al., 1996) to earlier periods. The history of opal deposition off the Zaire River is of interest (Schneider, 1991), as well as the origin of cycles of carbonate, organic matter deposition, and diatoms in each region.

- Determine what kind of oceanographic changes occur simultaneously in the Atlantic Ocean (Agulhas Current, polar front position, Equatorial Current, Argentine Current) with the shifting of the Benguela Current. Results from Ocean Drilling Program (ODP) Legs 108 and 114 can help define the past equatorial and polar boundaries of the Benguela Current. The final aim is to reconstruct the late Neogene paleocirculation pattern of the South Atlantic Ocean to evaluate implications for the glacial/interglacial heat balance through time between the South and North Atlantic. Of special interest is the identification of changes in modes of circulation, as seen in changes in correlations between proxy variables, as a function of time.

- Determine if changes in the surface-current and upwelling patterns of the Benguela Current cause, or are related to, changes in climates of western South Africa. For example, is the origin of the Namib Desert related to the initiation of upwelling activity off southwest Africa? Sites close to the continent probably contain enough information (clay minerals, grain size of terrigenous material, pollen, phytoliths, and freshwater diatoms) to allow reconstruction of continental climatic changes and to determine whether these changes are synchronous with oceanographic changes (i.e., the establishment of upwelling regions off southwest Africa).

- Examine the effect, if any, of sea-level changes on sedimentation below the Benguela Current. Published eustatic sea-level curves (Haq et al., 1987) will be useful for this purpose.

- Study early diagenetic processes in environments with very high organic carbon and opal contents, which will offer an interesting contrast to the studies undertaken during Leg 112, off Peru (Suess, von Huene, et al., 1990). The upwelling sediments off the Peruvian active margin are deposited in forearc basins in a disturbed tectonic setting, whereas off Angola and Namibia, sedimentation occurs on a steadily sinking passive margin with quite stable conditions. Therefore, we expect a more continuous and longer record in comparison to the sites drilled off Peru, although the sedimentation rate might not be quite as high.

RESULTS

SITE 1075

Site 1075 is the deep-water drill site on a depth transect in the Lower Congo Basin (Fig. 1). It is located in 2995 m deep water in a complex environment dominated by (1) the freshwater input from the Congo River, (2) seasonal coastal upwelling activity and associated filaments and eddies moving offshore, and (3) incursions of open-ocean waters, especially from the South Equatorial Countercurrent. We expect a close tie-in of climatic records from the continent and the ocean in this area. In the fan-margin deposits, the intercalation of pelagic and terrigenous information provides an excellent opportunity for studying cross-correlations of climatic effects on land and at sea. Site 1075, in connection with the two sites (1076 and 1077) in the Lower Congo Basin, allows us to reconstruct the changing influence of Congo River coastal upwelling and open-ocean contributions to the dynamics of the region.

Sediments at Site 1075 consist of one lithostratigraphic unit composed entirely of greenish gray diatomaceous clay and nannofossil-bearing diatomaceous clay (Fig. 2). The section at Site 1075 is apparently continuous and of Pleistocene to upper Pliocene age (Fig. 3). The sediment is bioturbated and displays a gradual increase in lithification with depth, but no structural or lithologic change can be observed. The sediments have overall low calcium carbonate contents of generally less than 2.5 wt%. Biogenic portions of the sediment contain abundant diatoms with variable amounts of nannofossils, rare silicoflagellates, siliceous sponge spicules, phytoliths, and traces of radiolarian and foraminifer fragments. Sedimentation rates for the recovered sequence average 100 m/m.y.

Detailed comparisons between the magnetic susceptibility record generated on the multisensor track (MST) and the high-resolution color reflectance measured with the Minolta spectrophotometer demonstrated complete recovery of the sedimentary sequence down to 234 meters composite depth (mcd).

Calcareous microfossils are poorly preserved, particularly in the lower section. Siliceous microfossils are relatively unaffected by dissolution and are abundant throughout Hole 1075A. We were able to develop an integrated, high-resolution biostratigraphy for the site that is in agreement with paleomagnetic interpretations. No apparent reworking has been identified. Diatoms are represented by marine and freshwater taxa. Clay minerals show varying contributions of kaolinite. Fluctuations of freshwater diatom and phytolith assemblages and kaolinite reflect changing continental climatic conditions.

A complete magnetostratigraphy was determined at Site 1075 after alternating-field (AF) demagnetization at 20 mT (Fig. 3). All chrons from the Brunhes (C1n) to the onset of C2n (Olduvai) at 1.95 Ma could be identified. Magnetic intensity is low and decreases with depth, although no decreasing trend was observed in the magnetic susceptibility. This suggests that the magnetic minerals that carry the remanent magnetization differ from those that dominate the magnetic susceptibility.

Interstitial water profiles record the complete consumption of sulfate at 30 meters below seafloor (mbsf), commensurate with increases in alkalinity and ammonium, all of which record the degradation of the high levels of sedimentary organic matter. The distribution of dissolved strontium, calcium, and magnesium suggests that the uppermost 50 mbsf is a region of calcite dissolution and dolomite precipitation. A sharp 2%-3% increase in the measured values of dissolved chloride through the upper 20 mbsf appears to reflect a stacked and damped diffusional signal of glacial seawater. We found no chemical evidence of methane hydrate at any depth at Site 1075.

The average concentration of total organic carbon (TOC) is 2.6%, which is rather high for ocean margin areas and reflects a history of elevated primary production in this area. The organic matter appears to be mostly marine in origin. Its microbial degradation in the sediments has fueled a sequence of redox processes. One consequence of the degradation has been the production of moderate amounts of biogenic methane and carbon dioxide and additional dissolution of

calcareous sediment components within the sediment.

Physical sediment properties were determined both by high-resolution MST core logging and index properties measurements. Magnetic susceptibility (Fig. 3) and gamma-ray attenuation porosity evaluator (GRAPE) signals reveal pronounced cyclicities. The high-resolution multichannel seismic record, which was acquired during the presite survey, reveals a reflection pattern that seems to be overprinted by in situ chemical or physical conditions not reflected in core log data. Clathrates, dissolved gas, or pore-pressure anomalies are potential explanations. High gas concentrations (CO_2 and methane) were found mainly in the interval of higher reflectivity beneath 100 mbsf.

Highlights of Site 1075 results include complete recovery of an apparently continuous Quaternary record, with a chance for extensive reconstruction of the response of the regional system to climatic forcing. First indications are that all major Milankovitch cycles are represented within the record, but with different spectral power depending on the type of record. For example, a strong 100-k.y. signal may be present in magnetic susceptibility in the upper Quaternary sediment, whereas a strong precessional signal appears in the red/green ratio in sediment reflectancy.

SITE 1076

Site 1076 is the shallow-water drill site on a depth transect in the Lower Congo Basin (Fig. 1). It is located in 1402 m deep water in a complex environment dominated by (1) the freshwater input from the Congo River, (2) seasonal coastal upwelling activity and associated filaments and eddies moving offshore, and (3) incursions of open-ocean waters, especially from the South Equatorial Countercurrent. We expect a close tie-in of climatic records from the continent and the ocean in this area. In the fan-margin deposits, the intercalation of pelagic and terrigenous information provides an excellent opportunity for studying cross-correlations of climatic effects on land and at sea. Site 1076, in connection with Sites 1075 and 1078 in the Lower Congo Basin, will allow us to reconstruct the changing influence of Congo River coastal upwelling and open-ocean contributions

to the dynamics of the region.

Drilling at Site 1076 recovered a relatively continuous hemipelagic sedimentary section spanning the last 1.5-1.6 m.y. of the Pleistocene. The sediments form one lithostratigraphic unit composed of bioturbated organic carbon-rich olive-gray clay and greenish gray clay (Fig. 2). Small shell fragments are present in many intervals. Above 150 mbsf, the calcium carbonate concentration alternates between 3 and 16 wt% and is limited below 150 mbsf to a maximum of 3.5 wt%. The biogenic portion of the sediment contains rare to abundant diatoms with rare nannofossils, silicoflagellates, siliceous sponge spicules, phytoliths, and traces of radiolarian and foraminifer fragments. Diatoms are abundant in both greenish gray and olive-gray intervals. Authigenic components are dominated by the presence of glauconite, dolomite, and iron sulfides. Rare, friable nodules, possibly phosphatic, are sometimes disseminated throughout certain intervals. Sedimentation rates range from 200 m/m.y. in the uppermost 80 mbsf, to 50 m/m.y. between 80 and 120 mbsf, to 210 m/m.y. between 120 and 200 mbsf.

Detailed comparisons between the magnetic susceptibility record generated on the MST and high-resolution color reflectance measured with the Minolta spectrophotometer demonstrated complete recovery of the sedimentary sequence down to 140 mcd.

Calcareous microfossils show evidence of reworking. Their abundance and preservation deteriorates gradually between 100 and 200 mbsf. Siliceous microfossils are relatively abundant, well preserved, and show no evidence of reworking. The calcareous nannofossil-based biostratigraphy is in disagreement with the paleomagnetic time frame for the lower half interval of Hole 1076A. We tentatively explain this discrepancy as a result of both poor preservation and reworking of calcareous nannofossils. Both calcareous nannofossil and benthic foraminifer assemblages suggest a discontinuity within the sedimentary record at a depth of 120 mbsf. Downcore changes in planktonic foraminifers and diatom assemblages are used as indices of variable surface and subsurface hydrography, as well as proxies for coastal upwelling and fluvial input.

A magnetostratigraphy was determined after AF demagnetization at 20 mT. The Matuyama/Brunhes boundary occurs at around 138 mbsf, and the onset and termination of the Jaramillo Subchron (C1r.1n) was identified in the lower part of the section. A short reversal event in the Brunhes Chron (possibly the Blake event) occurs in all four holes.

Interstitial water profiles record the complete consumption of dissolved sulfate within the uppermost 20 mbsf. In this interval alkalinity and ammonium also increase sharply, recording the degradation of organic matter. The distributions of dissolved strontium, calcium, and magnesium suggest two depth domains of carbonate dissolution and reprecipitation reactions: the first from 0 to 50 mbsf and the deeper from 120 to 200 mbsf.

The average concentration of TOC is 2.6%, which is rather high for ocean margin areas and reflects a history of elevated primary production in this area. The organic matter appears to be mostly marine in origin. Its microbial degradation in the sediments has fueled a sequence of redox processes. One consequence of the degradation has been the production of moderate amounts of biogenic methane and carbon dioxide and additional dissolution of calcareous sediment components within the sediment.

Physical sediment properties were determined both by high-resolution MST core logging and index properties measurements. Magnetic susceptibility and GRAPE signals reveal pronounced cyclicities, which were in conjunction with digital color data used for high-quality stratigraphic correlation.

Site 1076, through its position within the domain of Congo River sedimentation and its high-resolution continuous record back through much of the Quaternary, will provide the basis for a tie-in of climatic records of West Africa Congo River activity, coastal upwelling activity, and eastern tropical ocean dynamics. Of special interest are the competing source effects for land-derived materials, with some (most?) being brought directly by the river and the rest originating from reworked shelf sediments, especially during periods of low sea level.

SITE 1077

Site 1077 is the intermediate-water drill site on a depth transect in the Lower Congo Basin (Fig. 1). It is located in 2394 m deep water in a complex environment dominated by (1) the freshwater input from the Congo River, (2) seasonal coastal upwelling activity and associated filaments and eddies moving offshore, and (3) incursions of open-ocean waters, especially from the South Equatorial Countercurrent. We expect a close tie-in of climatic records from the continent and the ocean in this area. In the fan-margin deposits, the intercalation of pelagic and terrigenous information provides an excellent opportunity for studying cross-correlations of climatic effects on land and at sea. Site 1077, in connection with Sites 1075 and 1076 in the Lower Congo Basin, will allow us to reconstruct the changing influence of Congo River coastal upwelling and open-ocean contributions to the dynamics of the region.

Drilling at Site 1077 recovered a continuous hemipelagic sedimentary section spanning the entire Pleistocene (1.77 to 0 Ma). Sediments form one lithostratigraphic unit composed of intercalated, 40- to 150-cm-thick intervals of greenish gray diatom-rich, diatom-bearing, nannofossil-bearing, and nannofossil-rich clay (Fig. 2). The relative abundances of the biogenic components vary greatly with depth. Most of the sediment apparently is strongly bioturbated. Pteropod shells and small shell fragments are present in many intervals. Rare, friable nodules, possibly phosphatic, are interspersed throughout the sediment. The calcium carbonate contents varies between 0.8 and 13.2 wt%. The biogenic portions of sediments contain rare to frequent diatoms, rare nannofossils, silicoflagellates, siliceous sponge spicules, and phytoliths, and traces of radiolarian and foraminifer fragments. Authigenic components are dominated by the presence of glauconite, dolomite, and iron sulfides. X-ray diffraction analysis shows that the clastic fraction is dominated by smectite, kaolinite/illite, quartz, and minor amounts of albitic feldspar.

Detailed comparisons between the magnetic susceptibility record generated on the MST and high-resolution color reflectance measured with the Minolta spectrophotometer demonstrated complete recovery of the sedimentary sequence down to 183 mcd, with gaps in the continuous record at 25

and 125 mcd.

Calcareous microfossil abundance and preservation varies between the different groups and deteriorates with depth. Benthic foraminifers are abundant and well preserved down to 120 mbsf, calcareous nannofossils down to 130 mbsf, and planktonic foraminifers down to 150 mbsf. Siliceous microfossils are abundant and well preserved throughout the entire section. Both planktonic and benthic foraminifer assemblages display a major change at 52 mbsf. This change may represent a change in position of water masses at this location.

A magnetostratigraphy was determined after AF demagnetization at 20 mT. The Matuyama/Brunhes boundary occurs at around 120 mbsf, and the termination and onset of the Jaramillo Subchron (C1r.1n) was identified in the lower part of the section at around 130 and 140 mbsf, respectively.

Sediments average 2.3% TOC, which is rather high for ocean margin areas and reflects a history of elevated primary production in this area. Interstitial water chemistry studies document a sequence of diagenetic processes caused largely by the degradation of organic matter and carbonate dissolution/reprecipitation reactions. Among these are moderately high levels of methane and carbon dioxide generated by in situ microbial activity. These postdepositional processes are strongly similar to those found at nearby Sites 1075 and 1076 on the Congo Margin. A high-resolution study of interstitial water and headspace methane was conducted over the depth range at which a prominent seismic reflector exists to test whether this reflector is caused by methane hydrate. None of the profiles of salinity, dissolved chloride, or methane are characteristic of hydrate presence. There is no chemical evidence of the presence of methane hydrate in any portion of the sequence recovered from Site 1077.

Physical sediment properties were determined both by high-resolution MST core logging and index properties measurements. Magnetic susceptibility and GRAPE signals reveal pronounced cyclicities that were used for high-quality stratigraphic correlation in conjunction with digital color data.

Hole 1077A was logged with a limited suite of sensors to test the presence of gas hydrate as a potential cause of pronounced changes in seismic reflectivity between 80 and 120 mbsf to provide data for core-log integration and to obtain a continuous record as a proxy for paleoclimatic changes. The tool string included the spectral gamma-ray, long-spacing sonic, phasor dual induction, and Lamont high-resolution temperature (TLT) sondes. The hole was logged at 400 m/hr from 202 to 74 mbsf. The recorded data are of good quality, although density variations were within the resolution of the sensors and the sonic tool measured very low in situ velocities between 1470 and 1510 m/s. No anomalous data indicating hydrate accumulations were found at the reflector depths. Natural gamma-ray values correlate with core measurements and are valuable indicators of coring-induced deformation. The gamma-ray profile is correlated to the changing clay content of the sediment and clearly follows the glacial/interglacial stages of the oxygen-isotope record. Preliminary spectral analysis of the tuned natural gamma data shows a dominance of both the eccentricity and obliquity orbital cycles with a well-identified precessional signal.

On the whole, results from Site 1077 are similar to those from Site 1075, although with somewhat higher sedimentation rates for Site 1077. The shallower water depth at Site 1077 accounts for better preservation of calcareous fossils, especially in the upper portion of the sequence, where even pteropods (aragonite) were found in places. In combination with the high-resolution continuous 2-m.y. record of Site 1075, Site 1077 should greatly contribute to our understanding of the changing conditions of sedimentation in this area. Depositional patterns will reflect climatically driven changes in the supply of riverine materials (Congo), upwelling export (seasonal coastal upwelling), and open-ocean contributions. The Milankovitch-related cyclicity of the changes is evident already at this preliminary stage of analysis from inspection of a number of records.

SITE 1078

Site 1078 is located outside the Bight of Angola in 438 m deep water (Fig. 1). The site is part of a transect that will provide information on "pelagic background" sedimentation for the latest

Neogene, as it is situated between the high-productivity regions to the north and south. Sediments from this region indicate lower primary productivity in overlying waters compared to the adjacent upwelling areas. Thus, the influence of the open ocean is more pronounced and will provide a tie-in of coastal ocean history to the record of the pelagic environment. This will allow us to study the cross-correlations of climate-driven ocean dynamics across these two regimes. One of the intriguing aspects of this record is the low opal content associated with high organic matter accumulation. This paradox indicates there is a strong influence of subsurface waters, which originate elsewhere in the system, possibly in the subtropical convergence. Other topics of importance are the control of variation by precession, reflecting the changing dominance of trade wind and monsoonal effects.

A relatively continuous hemipelagic sedimentary section spanning the last 360 k.y. of the Pleistocene was recovered from Site 1078. Sediments at this site form one lithostratigraphic unit composed predominantly of a moderately bioturbated, olive-gray silty clay with varying amounts of nannofossils and foraminifers (Fig. 2). Sediments in the uppermost 3 m contain rare intact gastropod and mollusc shells, pteropods, and abundant shell fragments. Below 80 mbsf all holes contain several sections with whitish gray nodules, 1-2 mm in diameter. Diagenetic dolomite concretions between 3 and 7 cm thick and laminated intervals were found at various depths. Calcium carbonate varies between 1 and 25 wt%. The clastic fraction is dominated by smectite, kaolinite and/or illite, quartz, feldspar, and muscovite. The biogenic component is represented by frequent foraminifer fragments and nannofossils. Diatoms are abundant only in laminated sequences. Laminated packages also show abundant diatom resting spores. Trace amounts of plant remains and amorphous organic matter were observed occasionally.

Detailed comparisons between the magnetic susceptibility record generated on the MST and high-resolution color reflectance measured with the Minolta spectrophotometer demonstrated complete recovery of the sedimentary sequence down to 136 mcd.

Calcareous microfossils are abundant and well preserved in the entire section, except for the laminated intervals, which are barren of nannofossils. Both calcareous nannofossils and planktonic

foraminifers show evidence of reworking within the middle part of Hole 1078B. With the exception of the laminated intervals, diatoms, silicoflagellates, and radiolarians are absent at this site. The nannofossil-based biostratigraphy suggests that Site 1078 terminated within the upper half of Zone NN20, between 0.26 and 0.36 Ma.

Assuming a linear sedimentation rate between the two available datum events, sediments accumulated at a rate close to 600 m/m.y. for the interval from 0.09 to 0.26 Ma (Zone NN21a).

Magnetic inclinations and declinations after AF demagnetization at 20 mT from all four holes indicate that only the Brunhes (C1n) normal polarity chron is recorded. Short reversal events in the Brunhes Chron were not found despite the high sedimentation rates.

Sediments average 2.5% total organic carbon, which is rather high for ocean margin areas and reflects a history of elevated primary production in this area. Interstitial water chemistry studies document a sequence of diagenetic processes caused largely by the degradation of organic matter and carbonate dissolution/reprecipitation reactions. Among these are moderately high levels of methane and carbon dioxide generated by in situ microbial activity. These postdepositional processes are strongly similar to those found at Sites 1075, 1076, and 1077 on the Congo Margin. Profiles of salinity, dissolved chloride, and methane do not indicate the presence of gas hydrate in Site 1078 sediments.

Physical sediment properties were determined both by high-resolution MST core logging and index properties measurements. Magnetic susceptibility and GRAPE signals reveal pronounced cyclicities, which were used for high-quality stratigraphic correlation in conjunction with digital color data.

The site provides a good high-resolution record for the reconstruction of the oceanography of the eastern Angola Basin. Of special interest are the changing position of the Angola/Benguela Front and the supply of nutrients from the subsurface waters rising within the Angola Dome. The possibility that silicate content varies through time within that water must be considered; despite

high background productivity, the absence of diatoms is intriguing in this context. Much diatom dissolution takes place during early diagenesis, within a zone of high alkalinity generated by sulfate reduction. Occasional development of short laminated sequences (in one case cemented by dolomite) indicates sporadic oxygen deficiency in bottom waters. Possibly, such events are tied to change in the quality of upwelled waters, as suggested by the high abundance of diatoms within laminated sediments. Dolomite layers are present at some depths; several were found near 100 mbsf. Such layers may be important in determining the seismic reflectancy of sediments.

SITE 1079

Site 1079 is located outside the Bight of Angola in 749 m deep water (Fig. 1). The site is part of a transect that will provide information on "pelagic background" sedimentation for the latest Neogene, situated between the high-productivity regions to the north and south. Sediments from this region indicate lower primary productivity in overlying waters, compared to the adjacent upwelling areas. Thus, the influence of the open ocean is more pronounced and will provide a tie-in of coastal ocean history to the record of the pelagic environment. This will allow us to study the cross-correlations of climate-driven ocean dynamics across these two regimes. One of the intriguing aspects of this record is the low opal content associated with high organic matter accumulation. This paradox indicates a strong influence from subsurface waters, which originate elsewhere in the system, possibly in the subtropical convergence. Other topics of importance are the control of variation by precession, reflecting the changing dominance of trade wind and monsoonal effects.

Site 1079 recovered a relatively continuous hemipelagic sedimentary section spanning the last 700 k.y. of the Pleistocene (Fig. 2). Sediments form one lithostratigraphic unit composed predominantly of uniform olive-gray silty clay with varying amounts of nannofossils and foraminifers. There are also a few discontinuous light olive-gray silt laminae (1-2 mm thickness) which occur below 80 mbsf. Rare gastropods and frequent shell fragments are disseminated throughout the uppermost 60 mbsf. Whitish gray nodules, 1-2 mm in diameter, are sparse in some of the uppermost cores and become more frequent below 90 mbsf. The calcium carbonate

content ranges from 7 to 19 wt%, averaging about 13 wt%.

The silt component is dominated by smectite, kaolinite and/or illite, quartz, the feldspar minerals albite and microcline, and muscovite. The biogenic component is represented by frequent foraminifer fragments and nannofossils. Secondary minerals include dolomite, glauconite, and pyrite. Feldspar, in contrast to quartz, is not supplied by the Congo River but originates from igneous complexes in southern Africa and therefore probably represents a southern sediment source fed either by the Kunene River or eolian dust.

Sedimentation rates are high, around 400 m/m.y., in the uppermost 90 mbsf and are lower, around 50 m/m.y., between 90 and 120 mbsf.

Detailed comparisons between the magnetic susceptibility and the GRAPE density records generated on the MST demonstrated complete recovery of the sedimentary sequence down to 132 mcd.

Preservation of calcareous nannofossil specimens is good to very good. The overall abundance ranges from very abundant to abundant throughout the entire section. Reworked specimens (Neogene) are rare to common between 90 and 120 mbsf. Based on the oldest identified datum, the bottom age of Hole 1079A is estimated at 0.7 ± 0.05 Ma. The benthic foraminifers are well preserved and abundant at Site 1079; however, the diversity is relatively low and dominated by *Bolivina*. Planktonic foraminifers are common in the upper 50 mbsf, but abundance levels fall drastically below 60 mbsf. Diatoms, silicoflagellates, and radiolarians are absent.

Magnetic inclinations and declinations after AF demagnetization at 20 mT indicate that only the Brunhes (C1n) normal polarity chron is recorded. Short reversal events in the Brunhes Chron were not found, despite the high sedimentation rates.

Sediments average 3.0% TOC, which is high for ocean margin areas and reflects a history of elevated primary production in this area. Interstitial water chemistry studies document a sequence

of diagenetic processes in the upper 50 mbsf that are caused largely by the degradation of organic matter and carbonate dissolution/reprecipitation reactions. Among these are moderately high levels of methane and carbon dioxide generated by in situ microbial activity. Increases in interstitial water sulfate, chloride, and salinity from 70 mbsf to the bottom of Hole 1079A at 120 mbsf may reflect the influence of evaporite dissolution and brine formation. Profiles of salinity, dissolved chloride, and methane do not indicate the presence of gas hydrate in Site 1079 sediments.

Physical sediment properties were determined both by high-resolution MST core logging and index properties measurements. Magnetic susceptibility and GRAPE signals reveal pronounced cyclicities that were used for high-quality stratigraphic correlation in conjunction with digital color data.

Site 1079 was drilled as a companion to Site 1078 to make an east-west transect in the eastern Angola Basin. High productivity is greatly favored by the supply of nutrients from subsurface waters, probably involving the Angola Dome. Changes in productivity should record the intensity of domal and coastal upwelling and, possibly, the movement of the Benguela/Angola Front. Variations in supply of marine water or terrigenous matter will track climate changes in the drainage basins supplying the sediment, as well as the rates of uplift along the Angolan coast. Such uplift could be because of salt tectonics below the shelf, stimulated by increasing amplitudes of sea-level change. If so, terrigenous influx should greatly increase in the last 1 m.y.

SITE 1080

Site 1080 in the Southern Angola Basin (Fig. 1) was selected to sample the northern end of the Angola/Namibia upwelling region. The site should complement results obtained from Site 1081 at the Walvis Ridge. It is not only important for reconstruction of the history of the Benguela Current and coastal upwelling migration, but also for its contribution to the climatic history of southern Africa. In addition to frequencies and phase of productivity variations, we expect to obtain information on dry/wet cycles in the drainage basin of the Cunene River. Of special interest in this

context is the relationship of such cycles to the northern monsoon.

Drilling at Site 1080 recovered a hemipelagic sedimentary section probably spanning about 1 m.y. in the Pleistocene. Sediments form one lithostratigraphic unit composed of moderately bioturbated, dark greenish gray to olive-gray, diatom-bearing, and diatom-rich silty clays with varying abundances of nannofossils and foraminifers (Fig. 2). The clastic fraction is dominated by coarse silt-sized, angular, mono- and polycrystalline quartz grains with rare feldspar (albite and microcline) and detrital apatite clasts, muscovite, smectite, kaolinite, and perhaps illite. The biogenic component is represented by frequent diatom fragments, foraminifer fragments, and nannofossils. Radiolarians, plant remains, and particulate organic matter are present in trace amounts. Authigenic minerals include rounded glauconitic peloids and framboidal pyrite.

Detailed comparisons between the magnetic susceptibility and GRAPE density records generated on the MST and high-resolution color reflectance demonstrated complete recovery of the sedimentary sequence down to 42 mcd.

Micropaleontological studies were carried out on core-catcher samples from Holes 1080A and 1080B. The downhole succession of nannofossil assemblages from both holes indicates that the sedimentary sequence is incomplete and disturbed, possibly by turbiditic deposition. A hiatus of at least 400 k.y. duration (Zone NN20 and upper part of Zone NN19) was identified within a disturbed interval from 12 to 25 mbsf. Planktonic foraminifers are dominated by *Globigerina bulloides*, a species characteristic for upwelling and a high-productivity indicator. Dissolution effects increase downhole, reducing the abundance of the planktonic foraminifers. The absence of *Neogloboquadrina pachyderma* may represent a change to warmer surface-water conditions, but it may also be an artifact of dissolution. Radiolarians are present throughout the section with an abundance that ranges from few to abundant. The preservation is good in all investigated samples, and no apparent reworking was identified. Diatom abundance ranges from few to abundant. In general, preservation is poor and diatom valves are fragmented. Silicoflagellates, opaline phytoliths, and sponge spicules are also present. Reworking is not evident. The presence of nonplanktonic diatoms in all core-catcher samples points to material derived from the shelf.

Upwelling species dominate. *Chaetoceros* resting spores are abundant in all samples and are accompanied by neritic (rare to few) and open-ocean species (trace to rare).

A magnetostratigraphy was determined after AF demagnetization at 20 mT. The Matuyama/Brunhes boundary occurs at both holes ~10 mbsf, and the onset and termination of the Jaramillo Subchron (C1r.1n) was identified in Hole 1080A at 41 and 51 mbsf, respectively. A short reversal event in the Matuyama Chron was identified at both holes. The relative shortness of the Brunhes Chron compared with the distance to termination of the Jaramillo Chron suggests that the upper Quaternary record is missing at this site.

Sediments average 2.4% total organic carbon, which is rather high for ocean margin areas and reflects a history of elevated primary production in this area. Interstitial waters were gathered at a frequency of one sample per section, allowing high-resolution study of diagenetic processes through the entire cored sequence. The presence of a dolomite layer at 50 mbsf, which terminated drilling, indicates rock-forming dolomitization within the last 1 m.y. at the site. The profiles of alkalinity, ammonium, phosphate, and sulfate in the upper 10 mbsf reflect degradation of organic matter, and the distributions of dissolved calcium, magnesium, and strontium indicate active calcite dissolution and dolomite formation. Throughout this upper interval, the concentration of sedimentary calcite decreases from 26 wt% to less than 5 wt%, and dissolved strontium concentrations increase. From 25 mbsf to the dolomite layer, calcium and magnesium concentrations remain stable. The absence of decreases in these cations indicates that the dolomite layer is no longer growing.

Physical sediment properties were determined both by high-resolution MST core logging and index properties measurements. Magnetic susceptibility and GRAPE signals reveal characteristic cyclicities that were used for high-quality stratigraphic correlation in conjunction with digital color data.

The original goal to obtain a high-resolution record of the northern end of the Angola/Namibia upwelling system was not achieved. Hard dolomite layers at a depth of 35 to 50 mbsf denied

recovery by APC and proved difficult to penetrate by XCB, as well. Also, we quickly discovered that the sedimentary sequence is incomplete at this site and that calcareous fossils have been largely dissolved below the upper portion of the sequence. We anticipate, nevertheless, interesting insights into the dynamics of the mid-Pleistocene climate revolution from this site, with an expanded section between the termination of the Jaramillo Chron and the onset of the Brunhes Chron.

SITE 1081

At Site 1081, a relatively continuous hemipelagic sedimentary section spanning the Holocene to upper Miocene (0-9 Ma) was recovered. Sediments at Site 1081 consist of two lithostratigraphic units (Fig. 2). Unit I is composed of olive-gray to black clays that contain varying amounts of diatoms, nannofossils, foraminifers, and radiolarians. Three subunits are defined based on the various abundances and types of microfossils in the sediments: nannofossil- and foraminifer-rich clay (0-77 mbsf), diatom-rich clay (77-230 mbsf), and nannofossil-rich clay (230-390 mbsf). Lithostratigraphic Unit II (390-452 mbsf) is composed of olive-gray clayey nannofossil ooze. The detrital component of the sediments is clay with rare silt-sized, angular and subangular, mono- and polycrystalline quartz grains, feldspar, and mica. Muscovite and biotite also are present in trace amounts. The biogenic component is represented by varying abundances of foraminifers, nannofossils, and diatoms. Varying amounts of particulate organic matter were observed. Authigenic minerals, such as glauconite, rare framboidal pyrite, and dolomite, were observed. Quartz, microcline, and albite, which are probably supplied by the wind, and opal show parallel low-amplitude variations in the Miocene and lower Pliocene sediments. In the upper Pliocene and Pleistocene sediments, the amplitudes are larger, and the above eolian components are partly or completely decoupled from each other. These features suggest that the eolian supply of terrigenous material was dominated mainly by the strength of the trade winds during the late Miocene and early Pliocene. The later variations may be more readily caused by changes in the position of the atmospheric circulation system. Sedimentation rates are fairly constant within the upper Miocene and lower Pliocene sequences (40 m/m.y.). Sedimentation rates within the upper Pliocene

sequences are the highest recorded at this site (90-150 m/m.y.) but are reduced at the Pliocene/Pleistocene boundary (70 m/m.y.).

Detailed comparisons between the magnetic susceptibility and the GRAPE density records generated on the MST demonstrated complete recovery of the sedimentary sequence down to 215 mcd.

Fine biostratigraphic resolution was achieved by integrating datums from all microfossil groups. Except for planktonic foraminifers, all microfossil groups show marked coeval fluctuations in abundance that are reflected in the lithology. Planktonic foraminifers are barren, rare, or replaced by pyrite from 105 mbsf to the bottom of the hole. Calcareous nannofossils are abundant and well preserved within the upper (0-77 mbsf) and lower parts of the section (147-452 mbsf). Samples between 77 and 147 mbsf are commonly barren or poor, and the calcareous nannofossils are heavily etched, although some nannofossil-rich sediments are found occasionally within short intervals. The biostratigraphy of the Neogene is poorly constrained because of the scarcity of index species. Diatom abundance increases substantially in the upper Pliocene and lower Pleistocene sediments and reaches a maximum in the upper Pliocene sediment, whereas overall abundance levels remain low in the upper Miocene and lower Pliocene sediments. This pattern resembles that of DSDP Site 532. The diatom assemblage consists of a mixture of upwelling-related and oceanic species. Upwelling-related species dominate the diatom assemblage during highest abundance times in the upper Pliocene sediments. They are not common in lower Pliocene and Miocene sediments where oceanic species tend to dominate. The diatom content in the sediments possibly reflects a varying nutrient supply that could be related to upwelling of nutrient-rich deeper waters and high biological productivity over the Walvis Ridge, especially in the late Pliocene.

A complete magnetostratigraphy was determined in the uppermost 120 mbsf of the APC section at Site 1081 after AF demagnetization at 20 mT. All chrons could be identified from the Brunhes Chron (C1n) to the termination of C2n (Olduvai Chron) at 1.77 Ma.

Well-developed nannofossil ooze/clay cycles, in which concentrations of $CaCO_3$ and organic

carbon vary between 1% and 53% and 1.4% to 8.2%, respectively, reflect fluctuations in the elevated marine production associated with the Benguela Current. Higher concentrations of organic carbon from 0 to 200 mbsf record higher productivities during the last 2 m.y. than those recorded earlier in the history of this upwelling system. The interstitial water chemical profiles at this deeply drilled site record a relatively shallow (0 to 80 mbsf) region affected by the diagenetic degradation of organic matter that results in sulfate consumption, as well as increases in alkalinity, ammonium, and phosphate. These changes are accompanied by calcite dissolution and dolomite precipitation, which are recorded by increases in dissolved strontium and decreases in dissolved magnesium and calcium. Additionally, the diatomaceous sequence in lithostratigraphic Subunit IB causes an increase in dissolved silica and a second peak in dissolved phosphate deeper in the sediments.

Physical sediment properties were determined both by high-resolution MST core logging and index properties measurements. Magnetic susceptibility and GRAPE signals reveal pronounced cyclicities that were used for high-quality stratigraphic correlation in conjunction with digital color data.

The geophysical downhole logs show well-identified levels of high velocity, resistivity, and density, attributed mainly to dolomitic layers (Fig. 4). The Formation MicroScanner (FMS) shows dolomitic layers and numerous conductive horizons that might be related to high-porosity assemblages of diatomaceous microfossils. Porosity, density, and natural gamma-radiation logs show high-frequency cyclical patterns that will be used as valuable indicators of paleoclimatic history and will provide an age estimate of the sediment until 2 Ma.

Site 1081, in 790 m deep water on the Walvis Ridge (Fig. 1), is the shallow-water drill site of the Walvis Ridge/Walvis Basin transect. The other anchors are DSDP Sites 532 and 362, in 1300 m water depth, and Sites 1082 and 1083. The DSDP sites are seaward of the upwelling center but contain an upwelling signal that has been transported by the Benguela Current. Site 1081 will give a better record of the upwelling itself. The transect, located above the carbonate compensation depth (CCD) in a passive-margin area with high sedimentation rates, will provide high-resolution records of these important processes and add important new dimensions to the records now

available. This transect, situated as it is on the only topographic high over which the Benguela Current passes, is central to the reconstruction of the history of the current.

SITE 1082

Site 1082 is located in 1280 m deep water about 120 km to the southeast of DSDP Site 532 within the Northern Cape Basin (Fig. 1). Together with Sites 1081 and 1083 and DSDP Sites 532 and 362, it is part of a transect that is central to the reconstruction of the history of the Benguela Current. Site 1082 is closest to the coast and is expected to contain a direct record of upwelling history in the Walvis Bay area. The DSDP sites are well seaward of the upwelling center but contain an upwelling signal that was transported to this location by the Benguela Current and its filaments and eddies. Compared to DSDP Site 532, which shows evidence of sediment redeposition, Site 1082 offers a more continuous and less disturbed sequence.

From Site 1082 an apparently continuous hemipelagic sedimentary section spanning the upper Miocene to Holocene (5.8-0 Ma) was recovered. The upper part of the succession is composed of moderately bioturbated, intercalated intervals of olive to black clays, which contain varying abundances of diatoms, nannofossils, foraminifers, and radiolarians (Fig. 2). Three subunits are defined based on the various abundances and types of microfossils in the sediments: nannofossil- and foraminifer-rich clay (0-112 mbsf), diatom-rich clay (112-369 mbsf), and nannofossil clay (369-475 mbsf). The underlying lithostratigraphic unit (475-590 mbsf) consists of homogeneous, greenish gray nannofossil ooze. The lithostratigraphy at Site 1082 can be correlated to the one identified at Site 1081. Differences between these two sites are the higher sedimentation rates (70-200 m/m.y.) and the better temporal resolution at Site 1082 compared to Site 1081. Sediments at Site 1082 also have higher abundances of nannofossils than those at Site 1081.

The detrital component of the sediments consists of clay with rare silt-sized, angular and subangular, mono- and polycrystalline quartz and feldspar grains. Muscovite and biotite are present in trace amounts. Dolomite rhombs are observed in the diatom-rich clay and the

nannofossil ooze. The biogenic component is represented by varying abundances of foraminifers (whole and fragments), nannofossils, diatoms, radiolarians, sponge spicules, and silicoflagellates.

Quartz, muscovite, and the feldspars microcline and albite, probably supplied by the wind, are present in relatively constant proportions in the upper Pliocene sediments. In the Pleistocene sediments, these windblown components were partly or completely decoupled, most strongly during the last 400 k.y. This observation, together with those from Site 1081, will be used to identify the continental source of windblown dust.

Detailed comparisons between the magnetic susceptibility and the GRAPE density records generated on the MST and the color reflectance measured with the Minolta spectrophotometer demonstrated complete recovery of the sedimentary sequence down to 141 mcd.

Fine biostratigraphic resolution was achieved by integrating datums from all microfossil groups. Calcareous nannofossils are abundant within the entire section. Planktonic foraminifers indicate upwelling activity at 70 mbsf, and downhole faunal variations indicate that a warm surface water current (Angola Current) reached the region in the past. Tropical to warm subtropical species appear at 36 mbsf. The surface water warming is associated with a decrease in upwelling, as indicated by a reduced abundance of *G. bulloides*. The benthic foraminifer fauna show high diversity throughout the entire section. The record of diatom abundance points to a substantial increase in deposition during the upper Pliocene and lower Pleistocene sediments, reaching a maximum in the upper Pliocene, followed by a decrease within the Pleistocene at about 1 Ma. Overall abundances are low or diatoms are absent in upper Miocene and lower Pliocene sediments. The diatom content at Site 1082 probably reflects a varying nutrient supply that could be related to upwelling of nutrient-rich deeper waters and high biological productivity, especially in the upper Pliocene sequence. The diatom assemblage is similar to Site 1081 and consists mainly of a mixture of upwelling-indicator species.

The polarity of the remanent magnetization was determined from the magnetic declinations and inclinations of APC cores (Fig. 5) and from the magnetic inclinations of XCB cores after AF

demagnetization at 20 mT. All chrons from the Brunhes (C1n) to the onset of C3An at ~6 Ma could be identified. A short reversal event (Cobb Mountain) was observed at all three holes within the Matuyama Chron. The Reunion event (2.14 to 2.15 Ma) occurs in Hole 1082C between about 196 and 197 mbsf.

Well-developed cycles, in which concentrations of $CaCO_3$ and organic carbon vary between 1% and 85% and <0.1% to 16.1%, respectively, reflect fluctuations in the elevated marine production associated with the Benguela Current. Higher concentrations of organic carbon from 0 to 260 mbsf record higher productivities during the last 2 m.y. than earlier in the history of this upwelling system. The interstitial water chemical profiles record a relatively shallow (0 to 20 mbsf) region in which diagenetic degradation of organic matter consumes sulfate and produces increases in alkalinity, ammonium, and phosphate that ultimately exceed those found at nearby Site 1081 on the Walvis Ridge. These changes are accompanied by calcite dissolution and dolomite precipitation, which are recorded by increases in dissolved strontium and decreases in dissolved magnesium and calcium.

Physical sediment properties were determined both by high-resolution MST core logging and index properties measurements. Magnetic susceptibility and GRAPE signals reveal pronounced cyclicities, which were used for high-quality stratigraphic correlation in conjunction with digital color data.

Logging in Hole 1082A is characterized by a regular hole size (diameter ~10 to 11 in.) with numerous small enlargements from 530 to 120 mbsf and by washout zones at the top and bottom of the logged interval. Thirteen dolomitic layers were identified in the downhole logs, characterized by very high velocity, resistivity, and density, and by low gamma-ray intensity. Dolomitic layers are present in the entire interval but are particularly concentrated in the lower half. The core and log measurements of natural gamma-ray intensity are very similar and can be used for detailed correlations between the core and log dataset. In Hole 1082A, log depth is similar to core depth. The logging data from Sites 1081 and 1082 show a reliable correlation.

We expect that glacial/interglacial climatic cycles are well developed at Site 1082 in terms of productivity, carbonate dissolution, and terrigenous sedimentation cycles. In addition, the sediments from Site 1082 will document the supply of minerals and plant remains from land as a function of changing climate and sea level. Together with the results of Site 532, the record of Site 1082 will allow the definition of offshore gradients and the high-resolution reconstruction of the intensity of the Benguela Current. We expect detailed information of the history of upwelling activity, both on the scale of glacial/interglacial and subMilankovitch cycles. Trends will be compared with the records north and south of Walvis Ridge to identify long-term changes in boundary conditions.

SITE 1083

Site 1083 is the deep-water drill site (2180 m) of the Walvis Ridge/Walvis Basin transect (Fig. 1), which includes Sites 1081 and 1082 and DSDP Sites 532 and 362. Because of low sedimentation rates, one of the main objectives at Site 1083 is to provide an extended APC record back in time. The greater water depth should also result in well-expressed carbonate cycles via cyclic dissolution intensity. In addition, this site is farthest from shore and should have the best representation of pelagic signals.

Site 1083 recovered a relatively continuous hemipelagic sedimentary section spanning the last 2.6 m.y. Sedimentation rates range from 6 to 14 cm/k.y. with the highest values located within the last 0.26 m.y. as well as between 0.8 and 0.96 Ma (from the onset of the Jaramillo Chron to the onset of the Bruhnes Chron). The sediments form one lithostratigraphic unit composed of moderately bioturbated clayey nannofossil ooze (Fig. 2). This unit has been subdivided into two subunits based on the changing abundance of diatoms, which become more abundant below 130 mbsf. The stratigraphic variation in diatom abundance and the lithostratigraphic definitions are comparable to those at Sites 1081 and 1082. A major characteristic of sediments at Site 1083 is the repeated occurrence of dark-light color cycles throughout the drilled sequence. Similar to Site 1082, the lighter colored cycles are more calcium carbonate rich compared to the adjacent, more clay-rich,

darker colored cycles. Clay-rich intervals are generally 60 to 150 cm thick and occur approximately every 2 to 5 m.

The detrital component of the sediments consists of clay with rare silt-sized, angular and subangular, mono- and polycrystalline quartz and feldspar grains. Muscovite and biotite are present in trace amounts. Grain sizes of identifiable detrital components are relatively constant. Authigenic minerals, such as framboidal pyrite and dolomite rhombs, are rare or present in trace abundances only. Carbonate minerals are generally rare to frequent in abundance and, at times, are common.

The biogenic fraction of the sediment revealed abundant to very abundant nannofossils, abundant to common foraminifer fragments, rare siliceous sponge spicules, and trace amounts of radiolarians and silicoflagellates. Diatom abundances vary from common to barren. The relative abundances of the biogenic components change frequently within one core. The intercalated dark olive-brown and black clay intervals have distinctly lower abundances of biogenic components and occasionally show higher abundances of silt-sized mono- and polycrystalline quartz grains.

An integrated biostratigraphic framework composed of both calcareous and siliceous microfossils was established, resulting in a well-constrained age model for Site 1083. Preservation of nannofossil specimens is good to very good. Calcareous nannofossils are abundant to very abundant throughout the entire section. The scarcity of a late Pliocene index species (*Discoaster*) is probably related to colder than average surface water temperatures (a combination of increased upwelling intensity and advection of subantarctic surface water) over the South African and Namibian continental margins during the last 500 k.y. of the Neogene. The changes in planktonic foraminifer species indicate a northward shift in position of the Benguela Current associated with a shift in Southern Ocean circulation, or a reduced seasonality in southerly penetration of the Angola Current. Alternatively, the biotic change may indicate increased advection of Southern Ocean water in the Benguela Current system, or a combination of all factors. Radiolarians are present throughout. In most of the investigated samples, radiolarians are abundant, and preservation is good. Diatom preservation is moderate. As was the case for Sites 1081 and 1082, the record of

diatom abundance points to high deposition rates during the late Pliocene and early Pleistocene. The diatom assemblage is similar to that at Sites 1081 and 1082 and consists mainly of a mixture of upwelling-indicators and oceanic species. Two middle- to high-latitude cold-water indicator species indicate periods of intensified Southern Ocean input into the Benguela Current system.

A complete magnetostratigraphy was generated at Site 1083 after AF demagnetization at 20 mT. All chrons from the Brunhes (C1n) to the termination of C2An.1n (Gauss) at 2.58 Ma could be identified.

Dark-light color cycles, in which concentrations of $CaCO_3$ and organic carbon vary between 17% and 82% and 0.7% and 7.5%, respectively, reflect fluctuations in the elevated marine production associated with the Benguela Current. Most interstitial water chemical trends are intermediate between the neighboring Walvis Sites 1081 and 1082. Sulfate is completely consumed within the upper 25 mbsf; both alkalinity and ammonium display strong increases through this depth range. The concentration of interstitial water strontium reaches a maximum that is two to three times higher than that observed at Sites 1081 and 1082, reflecting the greater availability of biogenic calcite at Site 1083.

Physical sediment properties were determined both by high-resolution MST core logging and index properties measurements. Magnetic susceptibility and GRAPE signals reveal pronounced cyclicities that were used for high-quality stratigraphic correlation in conjunction with digital color data. Detailed comparisons between the magnetic susceptibility and the GRAPE density records generated on the MST demonstrated complete recovery of the sedimentary sequence down to 218.1 mcd, with a gap between 46 and 47.5 mcd (Fig. 6).

Of the sites on the Walvis Ridge/Walvis Bay transect, Site 1083 stands out because of its excellent microfossil record, which comprises both calcareous (foraminifers and nannofossils) and siliceous fossils (diatoms and radiolarians). This will allow intercalibration of the messages contained in these various assemblages regarding the history of change in current upwelling and regimes. Together with the other sites of this transect, a very exact reconstruction of conditions should be

possible for the last 2.6 m.y. Intercalibration of physical properties (MST data and sediment color) and chemical stratigraphy ($CaCO_3$ and C_{org}) with well-constrained information from microfossils should be of special interest at this site.

SITE 1084

One of the main objectives at Site 1084 (Fig. 1) is to document the northward migration of the Benguela Current system from the Miocene to the Quaternary periods, as well as the shoreward and seaward migrations of the upwelling center. Filaments of cold, nutrient-rich waters from the coastal upwelling area extend well offshore and mix with low-productivity oceanic water, forming a zone of intermediate productivity at Site 1084. Because of high sedimentation rates, this site is expected to provide a high-resolution record. The close vicinity to the Luederitz upwelling cell should result in well-expressed organic carbon, diatom, and coccolith cycles via cyclic productivity intensity. In addition, this site is closest to the area with elevated primary production and should have the best representation of coastal upwelling signals. A close tie-in between pelagic and terrigenous sedimentation is expected within the slope record.

Drilling at Site 1084 recovered a relatively continuous hemipelagic sedimentary section spanning the last 4.7 m.y. Sediments form four lithostratigraphic units defined by the changes in the major lithology between clay and ooze (Fig. 2). The uppermost lithology is composed of moderately bioturbated, intercalated intervals of clays that contain varying abundances of diatoms, nannofossils, foraminifers, and radiolarians. Three subunits are distinguished based on microfossil type and abundance. The section continues downward with about 100 m of clay-rich nannofossil diatom ooze, diatomaceous nannofossil ooze, and clay-rich nannofossil ooze. The following 50-m-thick unit is comprised of clay with varying amounts of nannofossils and diatoms underlain by a unit consisting predominantly of clayey nannofossil ooze.

Several decimeter-thick intervals of dark, organic-rich clay layers occur between 120 and 410 mbsf. These horizons are characterized by lower carbonate contents that average just below 10

wt% and by higher organic carbon contents that range between 8 and 18 wt% when compared to the under- and overlying sediment layers. The detrital component of the sediments consists of clay with rare silt-sized, angular and subangular mono- and polycrystalline quartz grains. Subangular feldspar grains are present in trace amounts. Authigenic minerals include framboidal pyrite and dolomite rhombs in rare or trace amounts. The dark horizons generally contain slightly higher abundances of pyrite and exhibit significant compositional variations in the relative abundances of diatoms, foraminifers, and nannofossils. The biogenic component of the dark layers is commonly dominated by diatom resting spores.

Sedimentation rates range from 100 to 270 m/m.y. with highest values located within the last 1 m.y. (Fig. 7). A second episode of high sedimentation rate (170 m/m.y.) is associated with an upper Pliocene diatom-rich interval.

Detailed comparisons between the magnetic susceptibility and the GRAPE density records generated on the MST and color reflectance measured with the Minolta spectrophotometer demonstrated complete recovery of the sedimentary sequence down to 175 mcd.

An integrated biostratigraphic framework composed of both calcareous and siliceous microfossils was established, resulting in a well-constrained age model for Site 1084 (Fig. 7). Calcareous nannofossils are abundant within the top 280 mbsf and between 410 and 600 mbsf and provided 13 biohorizons that were constrained within an average depth interval of 3 m. Planktonic foraminifer zonation is difficult because of an absence of marker species and dissolution of planktonic foraminifers, particularly in the lower Pleistocene to upper Pliocene sediments. It is difficult to determine whether the absence of marker species is caused by ecological conditions or by selective dissolution. Both cool- and warm-water faunas are present in the same assemblages downcore and may indicate an increased contribution from cooler Southern Ocean waters. The benthic foraminifers are abundant and well preserved, and abundances correlate well with the different lithostratigraphic units. Radiolarians are abundant and well preserved in almost all samples examined. Diatom preservation is moderate throughout Hole 1084A. In contrast to the other sites, diatom abundances, although highly variable, remain moderately high throughout the

Pleistocene sediments. In addition to the "background" diatom assemblage composed of a mixture of upwelling-indicator and oceanic species, we recorded many more cold-water markers characteristic of the Southern Ocean than at Sites 1081, 1082, and 1083. The intervals of greatest diatom abundances in the late Pliocene are recorded by a mixed/*Thalassiothrix antarctica*-rich assemblage and may represent mat deposits similar to the ones discovered in the eastern equatorial Pacific during Leg 138. The fact that these *T. antarctica*-rich sediments occur during persistent subantarctic water-mass influence at Site 1084 may relate to more vigorous surface circulation leading to the development of stronger frontal systems, facilitating the concentration of the diatom mats and, consequently, greater mat flux.

A complete magnetostratigraphy was determined at Site 1084 after AF demagnetization at 20 mT (Fig. 7). All chrons from the Brunhes (C1n) to the latter part of the Gilbert (~4.4 Ma) were identified. No short polarity-reversal event during the Brunhes Chron was detected in spite of the high sedimentation rates.

Sediments at Site 1084 are notably rich in marine organic matter. Well-developed light-dark sediment color cycles, in which concentrations of $CaCO_3$ and organic carbon vary between 1% and 69% and 1.2% and 18%, respectively, record fluctuations in the elevated marine production associated with the Benguela Current. Higher concentrations of organic carbon from 0 to 392 mbsf indicate that productivity was higher during the last 2 m.y. than earlier in the history of this upwelling system.

Interstitial water chemistry profiles at this organic-carbon-rich site record some of the most extreme conditions of sediment diagenesis ever recovered in the history of DSDP and ODP drilling. Maximum values of alkalinity (172 mM) and ammonium (50 mM) are greater than those observed at any site, except Site 688, within the Peruvian upwelling system (Fig. 8). Sulfate is completely depleted within the uppermost 5 mbsf, which is much more rapidly than in any other Leg 175 site and speaks to the availability of oxidizable organic matter. These changes are accompanied by calcite dissolution and dolomite precipitation, as recorded in the calcium, magnesium, and strontium distributions.

Physical sediment properties were determined both by high-resolution MST core logging and index properties measurements. Magnetic susceptibility and GRAPE signals reveal pronounced cyclicities that were used for high-quality stratigraphic correlation in conjunction with digital color data.

Hole 1084A was logged with a full suite of sensors to continuously characterize the sedimentary changes through depth and to provide data for core-log integration. Hole conditions above 170 mbsf are poor with a regular increase of the hole size. Nineteen dolomitic layers and 114 organic-rich dark layers were identified from logging data. Natural gamma-ray intensity can be used for detailed core-log correlations and for correlation with Site 1082 in the Walvis Basin.

Based on pore-water chemistry and C_{org} concentrations, Site 1084 records by far the highest productivity of the sites drilled. This was expected, since the site is close to the most active upwelling cell along southwest Africa; that is, the Luederitz Bay. The sediments recovered will allow high-resolution documentation of the variability of coastal upwelling for the last ~4.7 m.y.

SITE 1085

One of the main objectives for drilling at Site 1085 (Fig. 1) was to help document the path and strength of the Benguela Current system from the Miocene to the Quaternary periods, as well as the shoreward and seaward migrations of the upwelling center. The upwelling center inside the Benguela Coastal Current is fed from the thermocline by South Atlantic Central Water, and its intensity is related to the position and intensity of the Benguela Current system. Filaments of cold, nutrient-rich waters from the coastal upwelling area extend as much as 600 km offshore. Here, cold water mixes with low productivity oceanic water, forming a zone of intermediate productivity. Site 1085 is located offside from the mouth of the Orange River, which has water year round and delivers additional terrigenous sediments. This effect should be more pronounced during times when the Benguela Current and coastal upwelling activity were of lower intensity than today, so

that sediments from ocean production were less dominant. A close tie-in between pelagic and terrigenous sedimentation is expected to be present within the slope record.

Drilling at Site 1085 recovered a relatively continuous hemipelagic sedimentary section spanning the last 15 m.y. Sediments form two lithostratigraphic units dominated by nannofossil ooze (Fig. 2). The uppermost unit has been subdivided into two subunits to reflect the decrease in foraminifer abundances downhole. The underlying unit is a reddish brown, microfaulted, and thinly laminated clay-rich nannofossil ooze. Graded, 2- to 17-cm-thick beds rich in foraminifer tests are present between 30 and 70 mbsf. Below 360 mbsf, pyrite is present as isolated fine sand-sized grains and below 420 mbsf as nodules up to 1 cm in diameter. The deepest core of Hole 1085A is interpreted as a slump block. It consists of a thinly laminated reddish to olive-brown nannofossil ooze. Packages of occasionally graded laminae within this unit are commonly microfaulted, convolutely layered, and folded. The detrital component in sediments at Site 1085 is dominated by clay and trace abundances of silt-sized, subangular mono- and polycrystalline quartz grains. Sedimentation rates range from 15 to 80 m/m.y., with the highest values located within the last 8 m.y.

Physical sediment properties were determined both by high-resolution MST core logging and index properties measurements. Detailed comparisons between the magnetic susceptibility generated on the MST and color reflectance measured with the Minolta spectrophotometer demonstrated complete recovery of the sedimentary sequence down to 289 mcd.

A biostratigraphic framework composed of both calcareous nannofossils and foraminifers was established resulting in a well-constrained age model for Site 1085. Calcareous nannofossils are abundant and well preserved throughout the entire section. Reworking is limited to the interval between 60 and 100 mbsf. The overall abundance of benthic foraminifers is high throughout the studied interval. The planktonic to benthic foraminifer ratio at this site is about ten times higher than at previous sites. Radiolarians are generally rare and show signs of dissolution in almost all samples. Radiolarian assemblages indicate that intermittent upwellings occurred through the last ~3 m.y. The presence of an Antarctic species indicates an occasional influence of cooler currents. Diatoms are rare or absent in most of the section. The interval between 89.17 and 127.45 mbsf

(upper Pliocene, 1.8-2.6 Ma) contains a mixed/*T. antarctica*-rich diatom assemblage, similar to the one found in upper Pliocene sediments at Site 1084. Dinoflagellate cysts are common in the upper Miocene sediments (6-10 Ma).

A complete magnetostratigraphy was determined at Site 1085 after AF demagnetization at 20 mT. All chrons from the Brunhes (C1n) to the earliest part of the Gilbert (~5.5 Ma) were identified, although the quality of the record was not good because of a severe magnetic overprint.

Sediments at Site 1085 contain small amounts of marine organic matter, with TOC concentrations fluctuating between 2.8% and nil. Concentrations of $CaCO_3$ are generally between 85% and 60%, but drop to 35% in sediments deposited during the Miocene carbonate crisis. Interstitial water chemistry is dominantly controlled by the low organic carbon and high carbonate concentrations in the sediment, which result in modest variations in the chemical gradients of many dissolved species. Alkalinity rises to a broad maximum of approximately 30 mM between 46 and 84 mbsf and subsequently decreases to the bottom of the hole. The deepest alkalinity value of 1.752 mM is by far the lowest (except for near-surface data) observed so far during Leg 175 and most likely reflects consumption via clay mineral formation. Sulfate is not completely consumed until 65 mbsf, which is also deep in comparison to previous Leg 175 sites. Carbonate and phosphate precipitation reactions throughout the sequence are also inferred from the profiles of dissolved calcium, magnesium, and phosphate.

Hole 1085A was logged with a full suite of sensors to continuously characterize the sedimentary changes through depth and to provide data for core-log integration. The recorded data are affected by poor hole conditions. Enlargements and washout zones were identified in the entire logged interval. Despite the adverse hole conditions, measurements such as resistivity, sonic velocity, natural gamma ray, and magnetic susceptibility provided reliable data and show well-expressed changes related to the various proportions of biogenic, clastic, and organic components.

Drilling at Site 1085 recovered a continuous high-resolution record with sedimentation rates of

around 50 m/m.y. The carbonate-rich sediments will allow the reconstruction of the position and intensity of the Benguela Current for the last 15 m.y., including the influence of water masses coming from the Indian Ocean and the Subantarctic Region.

SITE 1086

Site 1086 is located in the southernmost area of the Cape Basin in 780 m deep water (Fig. 1). The primary objective for drilling at this site was to explore the early history of the Benguela Current in the southern Cape Basin and to detect possible Agulhas Current influences. We expect to obtain information about the supply of warm water from the Indian Ocean, through the Agulhas Retroflection, and from the Subtropical Convergence Zone, which are nearby. Both warm-water and cold-water eddies can be shed from the retroflection and the front, but the position of the Subtropical Convergence Zone and the transport by the Benguela Current will be crucial in determining which is more likely to reach the location of the site. The site is also located close to the continent and should detect upwelling signals and signals from continental climates, as well as sea-level changes.

Drilling at Site 1086 recovered a relatively continuous section spanning the upper Miocene to lower Pleistocene. The upper Pleistocene record apparently is missing. Sediments form one lithostratigraphic unit and are composed of clay-rich nannofossil-foraminifer ooze, and foraminifer-nannofossil ooze, foraminifer-rich nannofossil ooze, and nannofossil ooze (Fig. 2). Most of the sediment is moderately bioturbated, and burrows range in diameter from 1 mm to over 1 cm. The detrital component is dominated by clay and trace abundances of silt-sized, subangular mono- and polycrystalline quartz grains. Authigenic minerals are rare or present in trace abundances. Pyrite is present as silt-sized aggregates of euhedral crystals or as framboids. The biogenic component in all smear slides consists of abundant to very abundant nannofossils. Foraminifers are abundant to common.

Sedimentation rates are around 35 m/m.y. between 120 and 200 mbsf (Miocene to lower Pliocene

sediments) and are much lower (20 m/m.y.) in the upper Pliocene and Pleistocene sediments.

Calcareous nannofossils and planktonic foraminifer datums are in good agreement. Siliceous microfossils are rare or absent in much of the core. A significant amount of tropical to subtropical planktonic foraminifer species between 140 and 150 mbsf may indicate a warming event or increased input from the warm Aghulhas Current. There are but few radiolarian species at 25 mbsf; this suggests a warm and low-productivity ocean. Dinoflagellate cysts are common in the upper Miocene sediment between 140 and 206 mbsf (~5.9-7.5 Ma).

Except for the uppermost 30 mbsf, the cores show significant coring-induced remagnetization. The magnetostratigraphic interpretation at Site 1086 is based mainly on the inclinations after AF demagnetization at 20 mT. All chrons from the Olduvai (C2n) to C4n (~7.5 Ma) were identified.

Detailed comparisons between the magnetic susceptibility records generated on the MST and color reflectance measured with the Minolta spectrophotometer demonstrated complete recovery of the sedimentary sequence down to 232 mcd.

Sediments at Site 1086 are low in marine organic matter, with TOC concentrations fluctuating between 3.6% and nil. Concentrations of $CaCO_3$ are generally between 85% and 75%. The interstitial water composition is dominantly controlled by the high carbonate content and low organic carbon concentrations in the sediments. The chemical gradients at Site 1086 are even more gradual than those found at the lithologically similar Site 1085. For example, sulfate is not completely consumed until 180 mbsf, which was the greatest depth observed during Leg 175, and the alkalinity maximum at 125 mbsf is only 17 mM. Carbonate and phosphate precipitation reactions are inferred from the profiles of dissolved calcium, magnesium, and phosphate.

Physical sediment properties were determined both by high-resolution MST core logging and index properties measurements. Magnetic susceptibility and GRAPE signals reveal pronounced cyclicities.

Although the Quaternary record is missing, a continuous record back into the upper Miocene was recovered. Sedimentation rates are high in the lower part of the section, into the lower Pliocene. Subsequently, rates drop until they reach zero in the lowermost Quaternary sediment. At the water depth near 800 m, the site records properties of (and activity within) the upper water layers in the Southern Cape Basin. Increased winnowing since the lower Pliocene section apparently is reflected in the drop in sedimentation rate and results in an increasing proportion of sand fraction in the younger sediments.

SITE 1087

Site 1087 is located in the southernmost area of the Cape Basin in 1383 m deep water. The primary objective for drilling at this site was to explore the Neogene history of the Benguela Current in the Southern Cape Basin and to detect possible Agulhas Current influences. We expect to obtain information about the supply of warm water from the Indian Ocean, through the Agulhas Retroflection, and from the Subtropical Convergence Zone, which are nearby. Both warm-water and cold-water eddies can be shed from the retroflection and the front, but the position of the Subtropical Convergence Zone and the transport by the Benguela Current will be crucial in determining which eddy type is more likely to reach the location of the site. The site is also located close to the continent and should detect upwelling signals and signals from continental climates, as well as sea-level changes.

Site 1087 was cored to 492 mbsf and recovered a relatively continuous section down to 430 mbsf spanning the last 9 m.y. Sedimentation rates range from 20 to 70 m/m.y. The bottom 70 m contain a middle Miocene to lower Oligocene package interrupted by at least two major discontinuities. The sediments form two lithostratigraphic units composed of nannofossil ooze with varying abundances of clay and foraminifers. The sediments strongly resemble the lithologies observed at Sites 1086 and 1085. The sequence most likely contains various unconformities. The uppermost lithostratigraphic unit (0-425 mbsf) consists of nannofossil ooze with varying amounts of foraminifers. Sandy nannofossil foraminifer ooze is present in 50- to 100-cm-thick beds in the

upper 45 m. These beds have generally sharp bases, grade upward into more clay-rich, olive foraminifer nannofossil ooze, and are interpreted as turbidites. The underlying unit (425-492 mbsf) is composed of 2- to 100-cm-thick horizons of foraminifer-bearing and foraminifer-rich nannofossil ooze. A large unconformity is identified by an erosional contact at 450 mbsf and by biostratigraphic evidence. Below the erosional contact are fine laminations that are microfolded with sharp upper and lower contacts.

The detrital component is dominated by clay and trace abundances of silt-sized, subangular mono- and polycrystalline quartz grains. Pyrite is present as silt-sized aggregates of euhedral crystals or as framboids.

A preliminary biostratigraphy was developed using calcareous nannofossils and planktonic foraminifers. The biogenic component of both lithostratigraphic units consists of abundant to very abundant nannofossils. Foraminifers are abundant to few. Siliceous spicules, dinoflagellate cysts, and radiolarian tests are present in trace abundances only in the upper Pliocene and Pleistocene sediments. Radiolarian species indicate generally low productivity under subtropical warm-water conditions. The radiolarian assemblages that are characterized by common *Cycladophora davisiana* suggest upwelling conditions for samples from 60 to 70 mbsf. The presence of an Antarctic species at 112 mbsf indicates an influence of cooler water masses.

As at Site 1085, the upper Pliocene sediment contains an interval with a mixed assemblage rich in *T. antarctica* that is composed of Southern Ocean species and warm oceanic species, with an approximate age of 1.9-2.8 Ma. Dinoflagellate cysts are common below 213 mbsf and between 262 and 338 mbsf.

APC cores experienced a significant coring-induced remagnetization with a radial inward direction. Only magnetic inclinations showed distinct polarity biases after AF demagnetization at 20 mT, which allowed an interpretation of the magnetic polarity sequence from Chrons C1n to C2Ar (~4 Ma).

Magnetic susceptibility and GRAPE wet bulk density data were measured at 5- and 10-cm intervals. The correlation of features present in the physical properties measurements of adjacent holes was used to demonstrate the completeness of the stratigraphic sequence between 0 and 214 mcd.

Sediments are carbonate rich and organic carbon poor. Interstitial water chemistry is dominantly controlled by the high carbonate and low organic carbon concentrations in the sediment, which results in modest variations in the chemical gradients of many dissolved species. Alkalinity rises to a broad maximum of approximately 30 mM between 60 and 126 mbsf and subsequently decreases downhole. Sulfate is not completely consumed until 60 mbsf. Carbonate and phosphate precipitation reactions throughout the sequence are also inferred from the profiles of dissolved calcium, magnesium, and phosphate. Among the three Cape Basin sites, Site 1087 is most similar to Site 1085 in its geochemical profiles.

Logging in Hole 1087C encountered serious problems when the tool got stuck while entering the pipe after the first run. Good-quality logs were recorded with the seismo-stratigraphy tool string. In the upper 300 m of the logged interval, downhole measurements show very homogeneous patterns. The lower part of the logged interval is characterized by more variations in physical records related to the carbonate vs. detrital content.

Site 1087 is the southernmost site of a north-south transect along the West African coast from the Congo to South Africa. Sediments at this site were deposited continuously over the last 9 m.y. and will permit the reconstruction of the advection of water masses from the Indian Ocean and the Subantarctic Region. Drilling at the site will provide important new data about early carbonate diagenesis and about the processes involving redeposition of sediments on the continental slope.

CONCLUSIONS

The principal goals of Leg 175 were to (1) determine the history of the Benguela Current for the late Neogene; (2) study the productivity history of upwelling activity off Angola and Namibia and the influence of the Zaire River, thereby extending available information about the late Quaternary to earlier periods; (3) determine what kind of oceanographic changes occur simultaneously in the Atlantic Ocean with the shifting of the Benguela Current; (4) determine if changes in the surface-current and upwelling patterns of the Benguela Current cause, or are related to, changes in climates of western South Africa; (5) examine the effect, if any, of sea-level changes on sedimentation below the Benguela Current; and (6) study early diagenetic processes in environments with very high organic carbon and opal contents, which will offer an interesting contrast to the studies undertaken during Leg 112, off Peru.

1. *Determination of the Benguela Current history for the late Neogene*: The relevant sites are Sites 1081 through 1087, from Walvis Ridge to the Southern Cape Basin. Together they provide an excellent record for the late Neogene. Changes in the strength of the current are reflected in the composition of microfossil assemblages and in productivity-related sediment properties. Both a long-term trend toward greater strength and ice-cap-related cycles were observed.

2. *Study the productivity history of upwelling off Angola and Namibia:* Different types of upwelling—domal (Angola Basin), estuarine-influenced (off the Congo River), and coastal (off Lüderitz) were identified. These have different dynamics and histories. The outstanding feature regarding coastal upwelling is the late Pliocene diatom acme, seen between Walvis Ridge and Southern Cape Basin.

3. *Determination of oceanographic changes that occur simultaneously in the Atlantic Ocean with the shifting of the Benguela Current:* The mid-Pliocene productivity step from low to high diatom production off South Africa is, in essence, synchronous with the building of Northern Hemisphere ice masses. NADW production is affected, as seen in the carbonate record. Details will emerge from comparison of Leg 175 records with those from the Ceara Rise.

4. *Determine if changes in the surface-current and upwelling patterns of the Benguela Current cause, or are related to, changes in climates of western South Africa:* Clues to aridity history in Namibia and South Africa are contained in windblown dust within sediments recovered from Walvis Ridge and from the Northern Cape Basin. Upwelling history and aridity history will be matched in detail in these sites.

5. *Examination of the effect, if any, of sea-level changes on sedimentation below the Benguela Current:* Sea-level changes are recorded, in part, in a number of sediment properties, including gamma-ray activity, magnetic susceptibility, and color. Analysis of clay mineral content will be necessary to tie down the details.

6. *Study early diagenetic processes in environments with very high organic carbon and opal contents:* Chemical activity from the degradation of organic matter is extremely strong in most of the sediments recovered. Some of the most extreme values for ammonia and alkalinity ever measured were found at Site 1084. High methane and carbon dioxide values were ubiquitous. Authigenic mineral formation includes dolomite, which forms lithified beds regionally, affecting acoustic properties of sediments and seismic reflectivity.

REFERENCES

Baker, P.A., and Kastner, M., 1981. Constraints on the formation of sedimentary dolomite. *Science*, 213:214-216.

Barnola, J.M., Raynaud, D., Korotkevich, Y.S., and Lorius, C., 1987. Vostok ice core provides 160,000-year record of atmospheric CO_2. *Nature*, 329:408-414.

Berger, W.H., and Keir, R.S., 1984. Glacial-Holocene changes in atmospheric CO2 and the deep-sea record. In Hansen, J.E., and Takahashi, T. (Eds.), *Climate processes and climate sensitivity: Geophysical Monograph* 29, American Geophysical Union, Washington, D.C., 337-351.

Berger, W.H., and Wefer, G., 1996. Central themes of South Atlantic circulation. *In* Wefer, G., Berger, W.H., Siedler, G., and Webb, D. (Eds.), *The South Atlantic: Present and Past Circulation*, Springer-Verlag, 1-11.

Berger, W.H., Bickert, T., Yasuda, M., and Wefer, G., 1996. Reconstruction of atmospheric CO_2 from the deep-sea record of Ontong Java Plateau: The Milankovitch Chron. *Geologische Rundschau*, 85:466-495.

Berger, W.H., Smetacek, V., and Wefer, G., 1989. Ocean Productivity and Paleoproductivity - An Overview. *In* Berger, W.H., Smetacek, V., and Wefer, G., (Eds.), *Productivity of the Ocean: Present and Past:* Dahlem Workshop Reports, J. Wiley & Sons, Chichester, 1-34.

Bickert, T., and Wefer, G., 1996. Late Quaternary deep water circulation in the South Atlantic: Reconstruction from carbonate dissolution and benthic stable isotopes. *In* Wefer, G., Berger, W.H., Siedler, G., and Webb, D., (Eds.), *The South Atlantic: Present and Past Circulation*, Springer-Verlag, 599-620.

Bolli, H.M., Ryan, W.B.F., et al., 1978. *Init. Repts. DSDP*, 40: Washington (U.S. Gov. Printing Office).

Boyle, E.A., and Keigwin, L., 1987. North Atlantic thermohaline circulation during the past 20,000 years linked to high-latitude surface temperature. *Nature*, 330:35-40.

Bremner, J.M., 1983. Biogenic sediments on the South West African (Namibian) continental margin. *In* Thiede, J., and Suess, E., (Eds.), *Coastal Upwelling, Its Sediment Record,* Part

B, Plenum Press, 73-103.

Calvert, S.E., and Price, N.B., 1983. Geochemistry of Namibian Shelf Sediments. *In* Suess, E., and Thiede, J. (Eds.), Coastal Upwelling, Its Sediment Record, Part A: *Responses of the Sedimentary Regime to Present Coastal Upwelling*, NATO Conference Series, Series IV: Marine Sciences, Vol. 10a: 337-375.

CLIMAP Project Members, 1976. The surface of the ice-age earth. *Science*, 191:1131-1137.

COSOD II, 1987. *Report of the Second Conference on Scientific Ocean Drilling*, Joint Oceanographic Institutions for Deep Earth Sampling, European Science Foundation. Strasbourg, 142 pp.

Diester-Haass, L., 1985. Late Quaternary sedimentation on the eastern Walvis Ridge, SE Atlantic (HPC 532 IPOD Leg 75) and neighbored piston cores. *Mar. Geol.*, 65:145-189.

Garrison, R.E., Kastner M., and Zenger, D.H. (Eds.), 1984. Dolomites of the Monterey Formation and other organic-rich units. Soc. Econ. Paleont. Mineral., Pacific Section, *Spec. Publ.* 41, 215 pp.

Haq, B.U., Hardenbol, J., and Vail, P.R., 1987. Chronology of fluctuating sea-levels since the Triassic. *Science*, 235:1156-1167.

Hay, W.W., Sibuet, J.C., et al., 1984. *Init. Repts. DSDP*, 75 (2 vols.): Washington (U.S. Govt. Printing Office).

Hodell, D.A., and Venz, K., 1992. Toward a high-resolution stable isotopic record of the Southern Ocean during the Pliocene-Pleistocene (4.8 to 0.8 Ma). *In* Kennett, J.P., Warnke, D.A., (Eds.), *The Antarctic Paleoenvironment: A Perspective on Global Change* Part One Vol 56 (Antarctic Research Series) American Geophysical Union, Washington D.C., 265-310.

Jansen, J.H.F., Ufkes, E., and Schneider, R.R., 1996. Late Quaternary Movements of the Angola-Benguela Front, SE Atlantic, and Implications for Advection in the Equatorial Ocean. *In* Wefer, G., Berger, W.H., Siedler, G., and Webb, D. (Eds.), *The South Atlantic: Present and Past Circulation*, Springer-Verlag, 553-575.

Kulm, L.D., Suess, E., and Thornburg, T.M., 1984. Dolomites in organic-rich muds of the Peru forearc basin: analogue to the Monterey Formation. *In* Garrison, R.E., Kastner, M., and Zenger, D.H. (Eds.), *Dolomites of the Monterey Formation and other organic-rich units: Pacific Section*, Soc. Econ. Paleont. Mineral., 41:29-47.

McIntyre, A., Ruddiman, W.F.K., Karlin, K., and Mix, A.C., 1989. Surface water response of the equatorial Atlantic Ocean to orbital forcing. *Paleoceanography*, 4:19-55.

Millero, F.J., and Sohn, M.L., 1992, *Chemical Oceanography*, Boca Raton (CRC Press).

Oberhänsli, H., 1991. Upwelling signals at the northeastern Walvis Ridge during the past 500,000 years. *Paleoceanography*, 6:53-71.

Sarnthein, M., Duplessy, J.C., and Fontugne, M.R., 1988. Global variations of surface ocean productivity in low and mid latitudes; influence on CO_2 reservoirs of the deep ocean and atmosphere during the last 21,000 years. *Paleoceanography*. 3:361-399.

Schneider, R., 1991. Spätquartäre Produktivitätsänderungen im östlichen Angola-Becken: Reaktion auf Variationen im Passat-Monsun-Windsystem und in der Advektion des Benguela-Küstenstroms. *Berichte Fachbereich Geowissenschaften* Nr. 21, 198 S.

Schneider, R.R., Müller, P.J., Ruhland, G., Meinecke, G., Schmidt, H., and Wefer, G., 1996. Late Quaternary Surface Temperatures and Productivity in the East-Equatorial South Atlantic: Response to Changes in Trade/Monsoon Wind Forcing and Surface Water Advection. *In* Wefer, G., Berger, W.H., Siedler, G., and Webb, D. (Eds.), *The South Atlantic: Present and Past Circulation*, Springer-Verlag, 527-551.

Shackleton, N.J., et al., 1984. Oxygen isotope calibration of the onset of ice-rafting and history of glaciation in the North Atlantic region. *Nature*, 307:620-623.

Suess, E., von Huene, R., et al., 1990. *Proc. ODP, Sci. Results*, 112: College Station, TX (Ocean Drilling Program).

Sundquist, E.T., and Broecker, W.S., 1985. The carbon cycle and atmospheric CO_2: natural variations Archean to Present. *American Geophysical Union, Monograph*, 32.

Vincent, E., and Berger, W.H., 1985. Carbon dioxide and polar cooling in the Miocene: the Monterey hypothesis. *In* Sundquist, E.T., and Broecker, W.S. (Eds.), *The Carbon Cycle and Atmospheric CO_2: Natural Variations Archean to Present*, Geophysical Monograph 32, 455-468.

Wefer, G., Berger, W.H., Bickert, T., Donner, B., Fischer, G., Kemle-von Mücke, S., Meineck, G., Müller, P.J., Mulitza, S., Niebler, H.-S., Pätzold, J., Schmidt, H., Schneider, R.R., and Segl, M., 1996. Late Quaternary surface circulation in the South Atlantic: The stable isotope record and implications for heat transport and productivity. *In* Wefer, G., Berger,

W.H., Siedler, G., and Webb, D.,(Eds.), *The South Atlantic: Present and Past Circulation*, Springer-Verlag, 461-502.

FIGURE CAPTIONS

Figure 1. Overview map showing general working areas and locations of Sites 1075 to 1087.

Figure 2. Lithostratigraphic summary profiles for all sites drilled during Leg 175.

Figure 3. Composite stratigraphic section for Site 1075 showing core recovery in all holes, a simplified summary of lithology, age, paleomagnetics, color reflectance, magnetic susceptibility, and calcium carbonate content.

Figure 4. Downhole logs of caliper, natural gamma ray, resistivity, density, velocity, magnetic susceptibility, and uranium content from Hole 1081A.

Figure 5. Remanent magnetization: intensity, declination, magnetostratigraphic interpretation, and inclination after AF demagnetization at 20 mT for Hole 1082C. The light gray plots in the declination column represent nonoriented cores.

Figure 6. The composite section for Site 1083. Magnetic susceptibility and GRAPE density are plotted for Holes 1083A (thick black line), 1083B (gray line), 1083C (dotted line), and 1083D (thin black line). The downhole logs are shown in meters composite depth (mcd). A constant has been added to susceptibility and GRAPE to offset the line plots.

Figure 7. Depth-age plot and sedimentation rates (cm/k.y.) estimated from calcareous microfossil (open circles; F = planktonic foraminifers, N = calcareous nannofossils) and siliceous microfossil (closed circles; D = diatoms, R = radiolarians, S = silicoflagellates) datums in Hole 1084A.

Figure 8. Downcore profiles of dissolved alkalinity, ammonium, and sulfate at Site 1084. Lithostratigraphic subunits are shown on right-hand bar. Arrows on relevant axes indicate mean ocean-bottom water values taken from Millero and Sohn (1992).

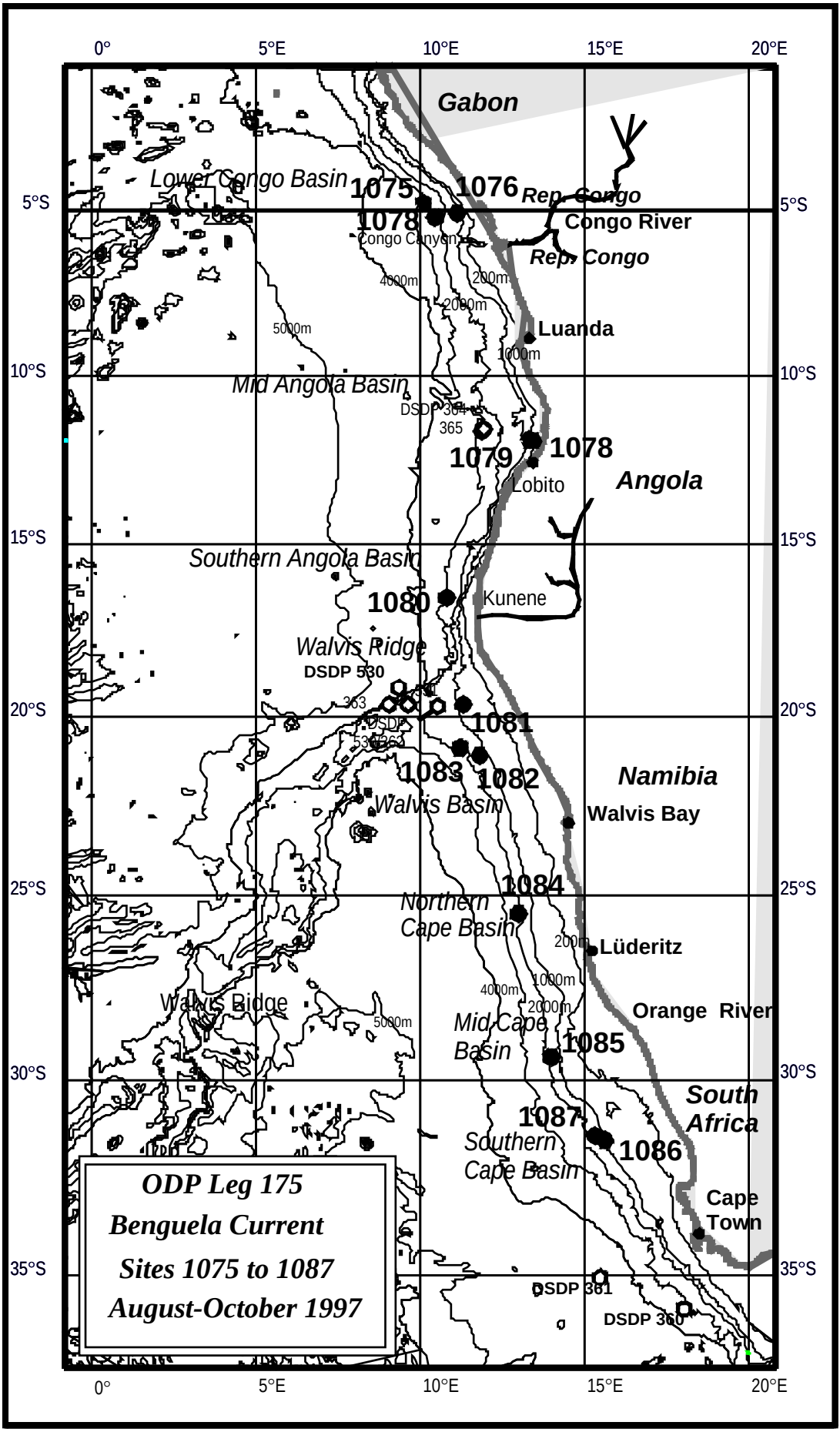
0°
5°E
10°E
15°E
20°E
5°S
10°S
15°S
20°S
25°S
30°S
35°S
Gabon
Lower Congo Basin
1075
1076
Rep. Congo
1078
Congo River
Congo Canyon
Rep. Congo
4000m
2000m
200m
5000m
Luanda
1000m
Mid Angola Basin
DSDP 364
365
1079
1078
Lobito
Angola
Southern Angola Basin
1080
Kunene
Walvis Ridge
DSDP 530
363
DSDP
530/363
1081
1083
1082
Namibia
Walvis Basin
Walvis Bay
1084
Northern
Cape Basin
200m
Lüderitz
4000m
1000m
2000m
Walvis Ridge
5000m
Orange River
Mid Cape
Basin
1085
South
Africa
1087
Southern
Cape Basin
1086
Cape
Town
DSDP 361
DSDP 360
ODP Leg 175
Benguela Current
Sites 1075 to 1087
August-October 1997

Figure 1

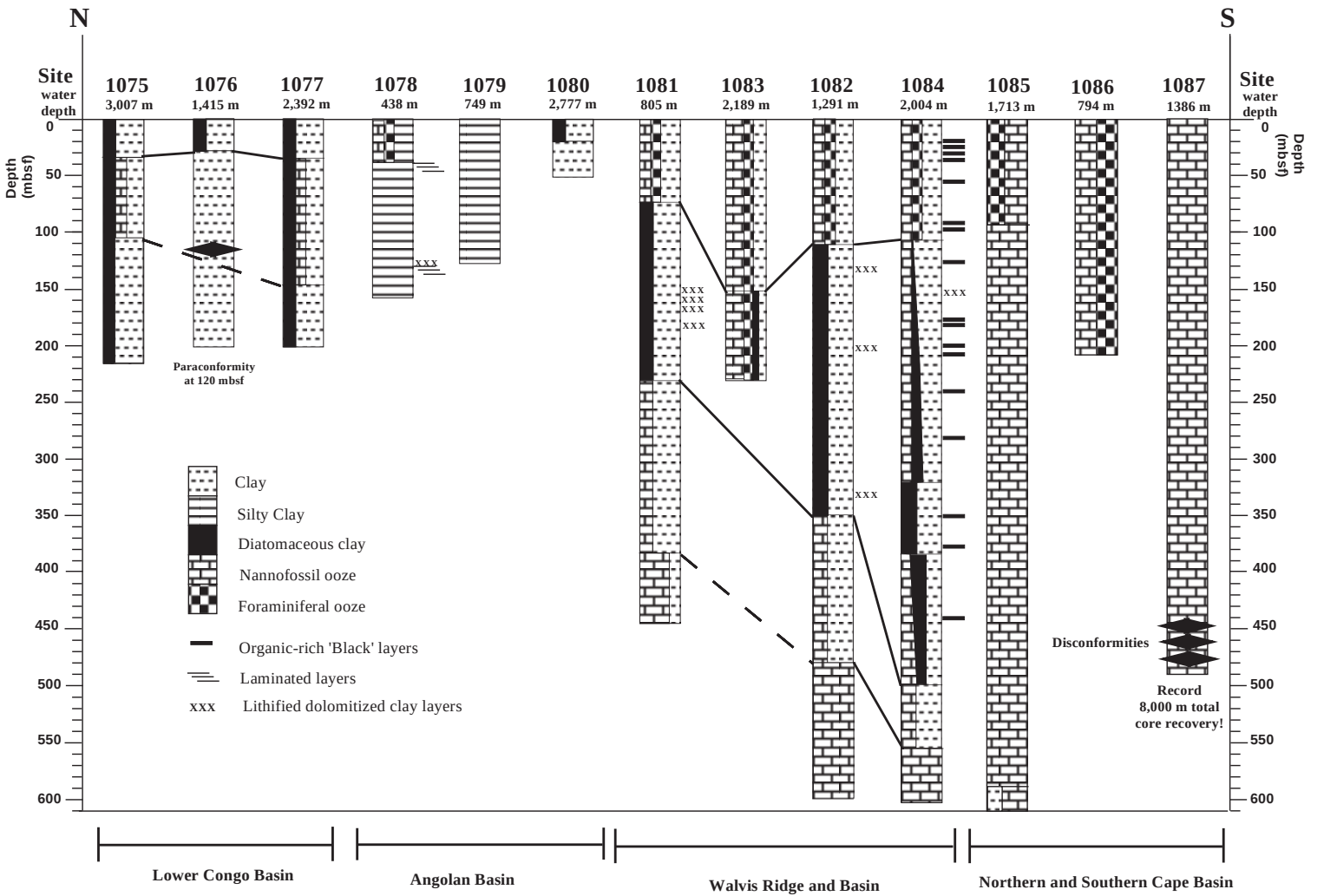
N
S
Site water depth
1075 3,007 m
1076 1,415 m
1077 2,392 m
1078 438 m
1079 749 m
1080 2,777 m
1081 805 m
1083 2,189 m
1082 1,291 m
1084 2,004 m
1085 1,713 m
1086 794 m
1087 1386 m
Depth (mbsf)
0
50
100
150
200
250
300
350
400
450
500
550
600
Paraconformity at 120 mbsf
Clay
Silty Clay
Diatomaceous clay
Nannofossil ooze
Foraminiferal ooze
Organic-rich 'Black' layers
Laminated layers
xxx Lithified dolomitized clay layers
Disconformities
Record 8,000 m total core recovery!
Lower Congo Basin
Angolan Basin
Walvis Ridge and Basin
Northern and Southern Cape Basin

Figure 2

Leg: 175 Site: 1075

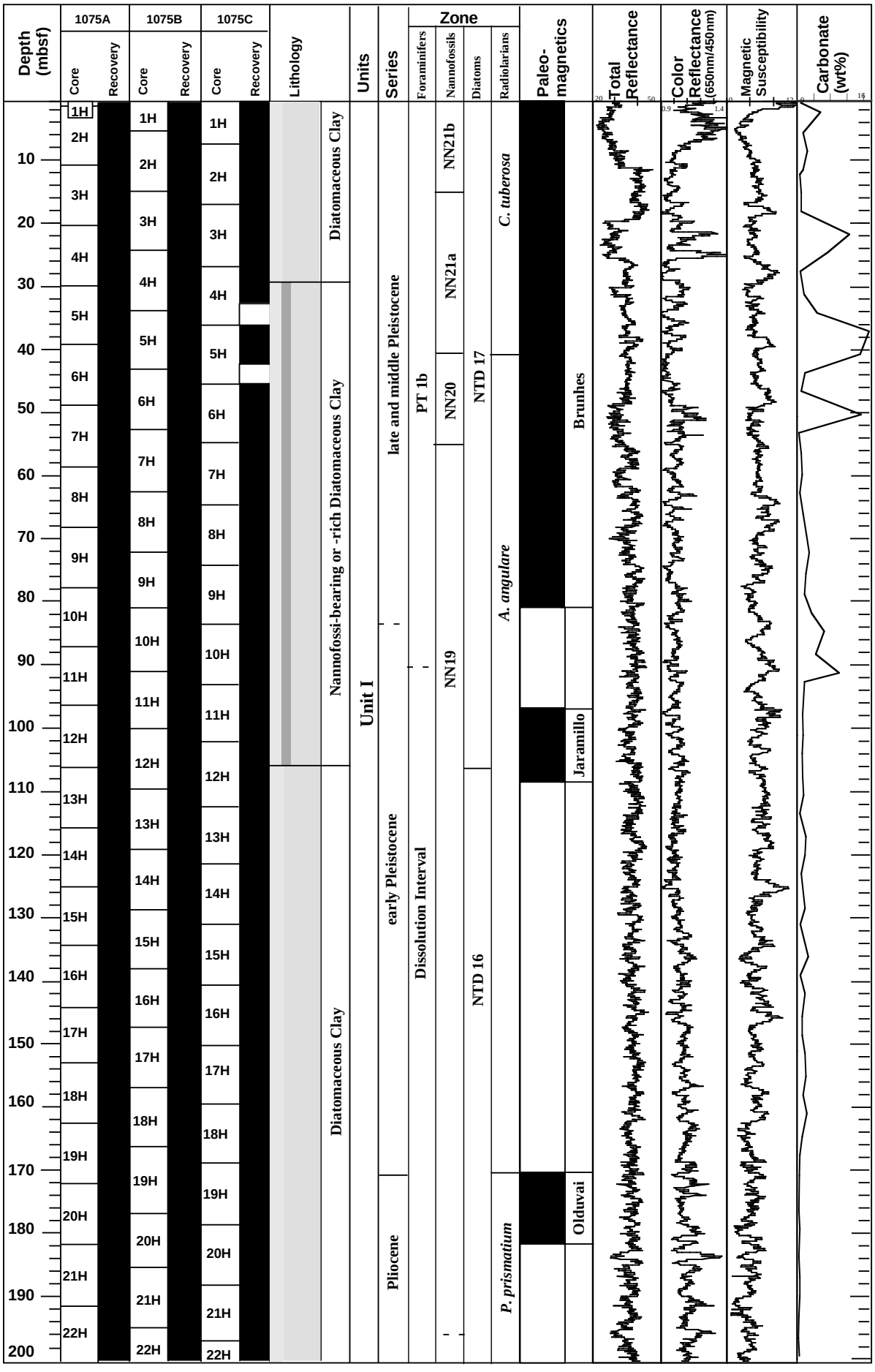

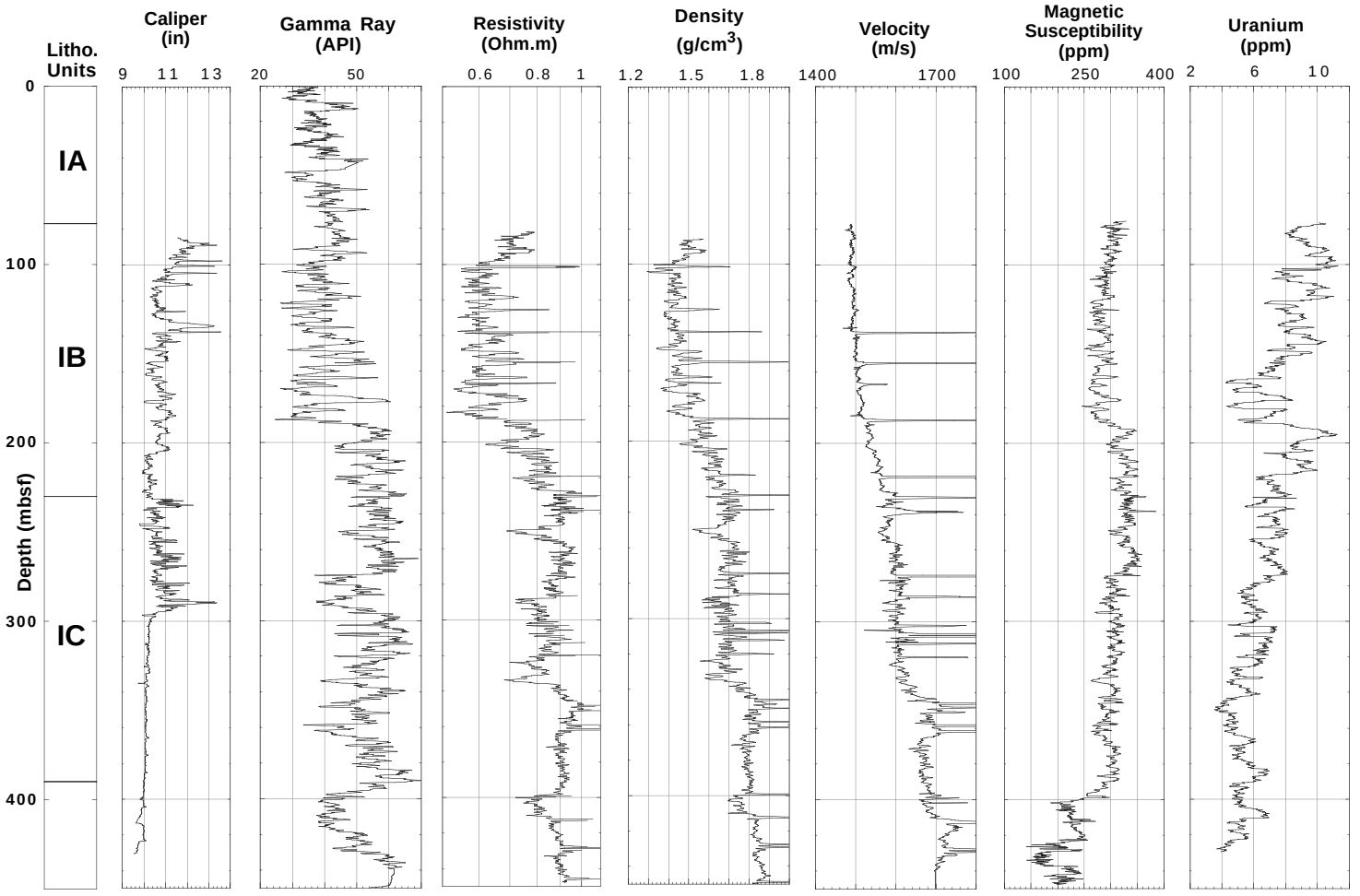
Litho. Units
Caliper (in)
9 11 13
Gamma Ray (API)
20 50
Resistivity (Ohm.m)
0.6 0.8 1
Density (g/cm3)
1.2 1.5 1.8
Velocity (m/s)
1400 1700
Magnetic Susceptibility (ppm)
100 250 400
Uranium (ppm)
2 6 10
Depth (mbsf)
0
100
200
300
400
IA
IB
IC

Figure 4

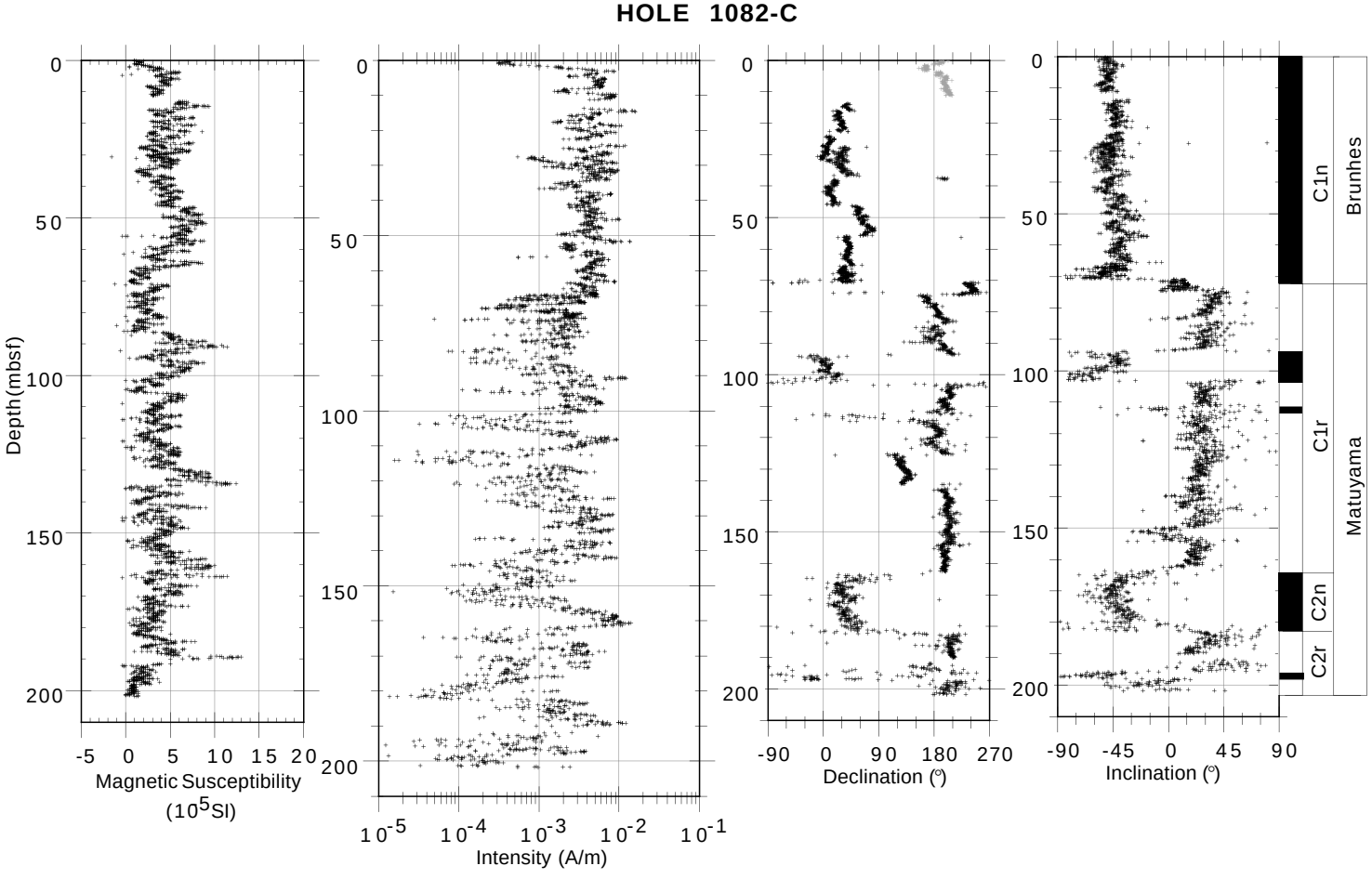
HOLE 1082-C
Depth(mbsf)
0
50
100
150
200
-5 0 5 10 15 20
Magnetic Susceptibility
(10^5SI)
10^-5 10^-4 10^-3 10^-2 10^-1
Intensity (A/m)
-90 0 90 180 270
Declination (°)
-90 -45 0 45 90
Inclination (°)
C1n
Brunhes
C1r
Matuyama
C2n
C2r

Figure 5

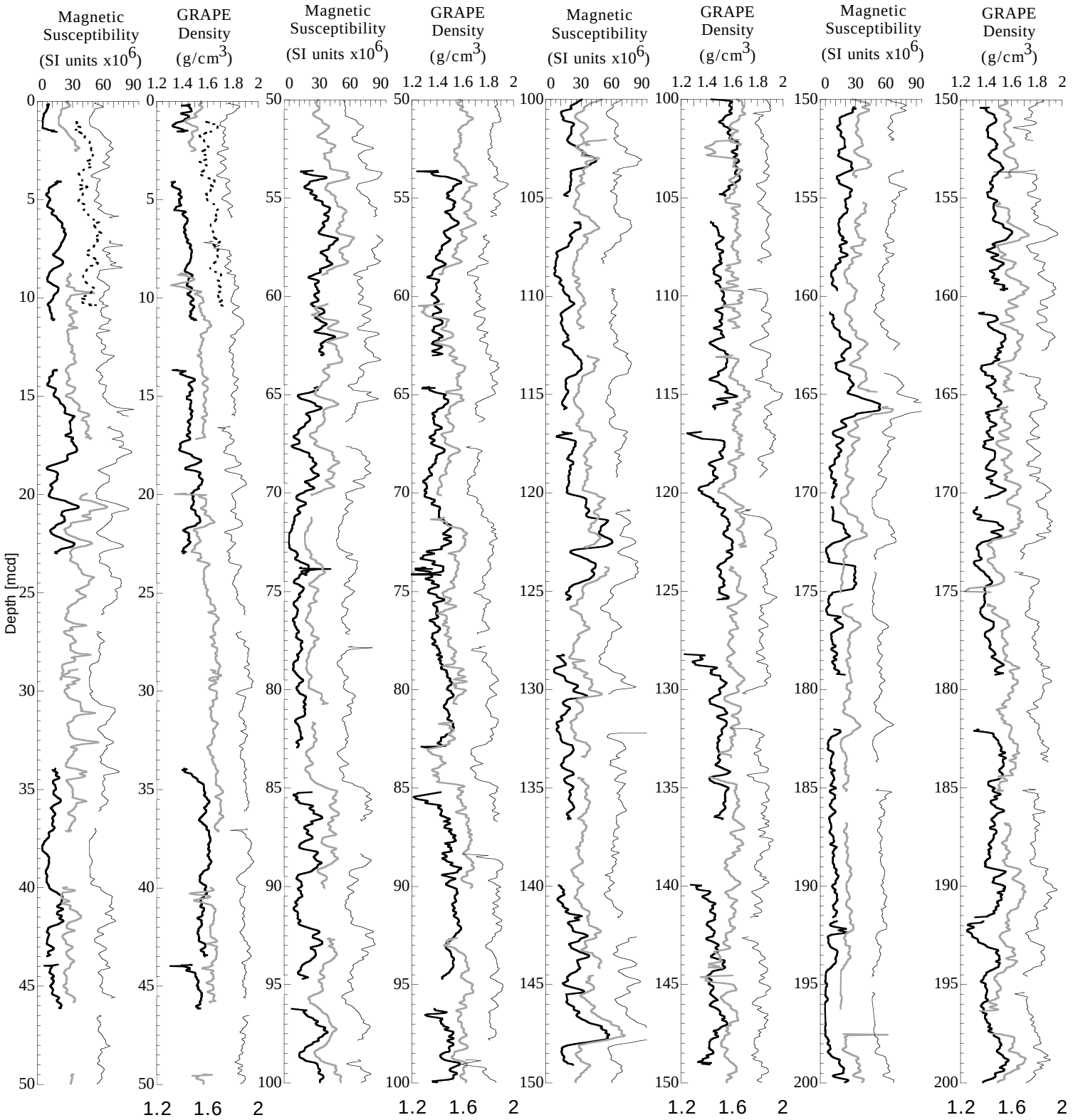
Magnetic Susceptibility (SI units x10^6)
GRAPE Density (g/cm^3)
Depth [mcd]

Figure 6

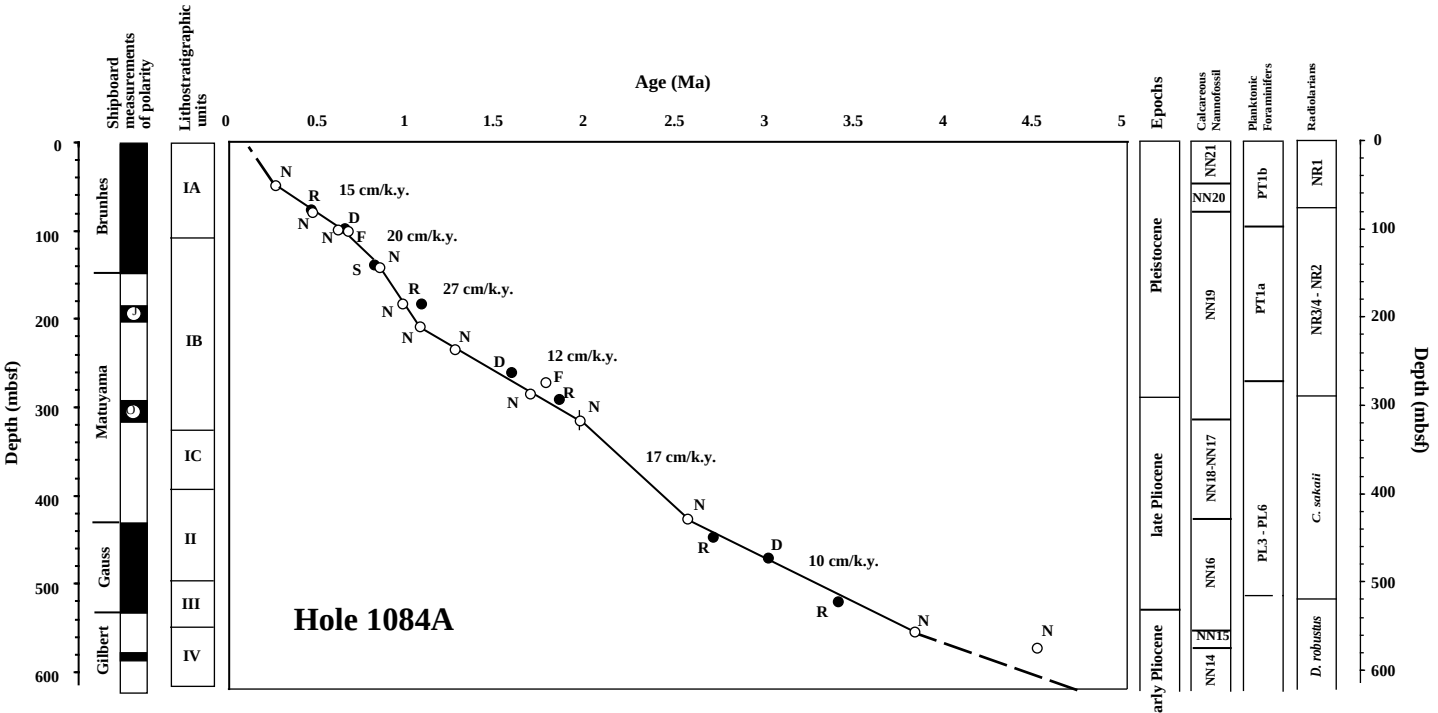
Depth (mbsf)
0
100
200
300
400
500
600
Shipboard measurements of polarity
Brunhes
Matuyama
Gauss
Gilbert
Lithostratigraphic units
IA
IB
IC
II
III
IV
Age (Ma)
0
0.5
1
1.5
2
2.5
3
3.5
4
4.5
5
15 cm/k.y.
20 cm/k.y.
27 cm/k.y.
12 cm/k.y.
17 cm/k.y.
10 cm/k.y.
Hole 1084A
Epochs
Pleistocene
late Pliocene
early Pliocene
Calcareous Nannofossil
NN21
NN20
NN19
NN18-NN17
NN16
NN15
NN14
Planktonic Foraminifers
PT1b
PT1a
PL3 - PL6
Radiolarians
NR1
NR3/4 - NR2
C. sakaii
D. robustus
Depth (mbsf)

Figure 7

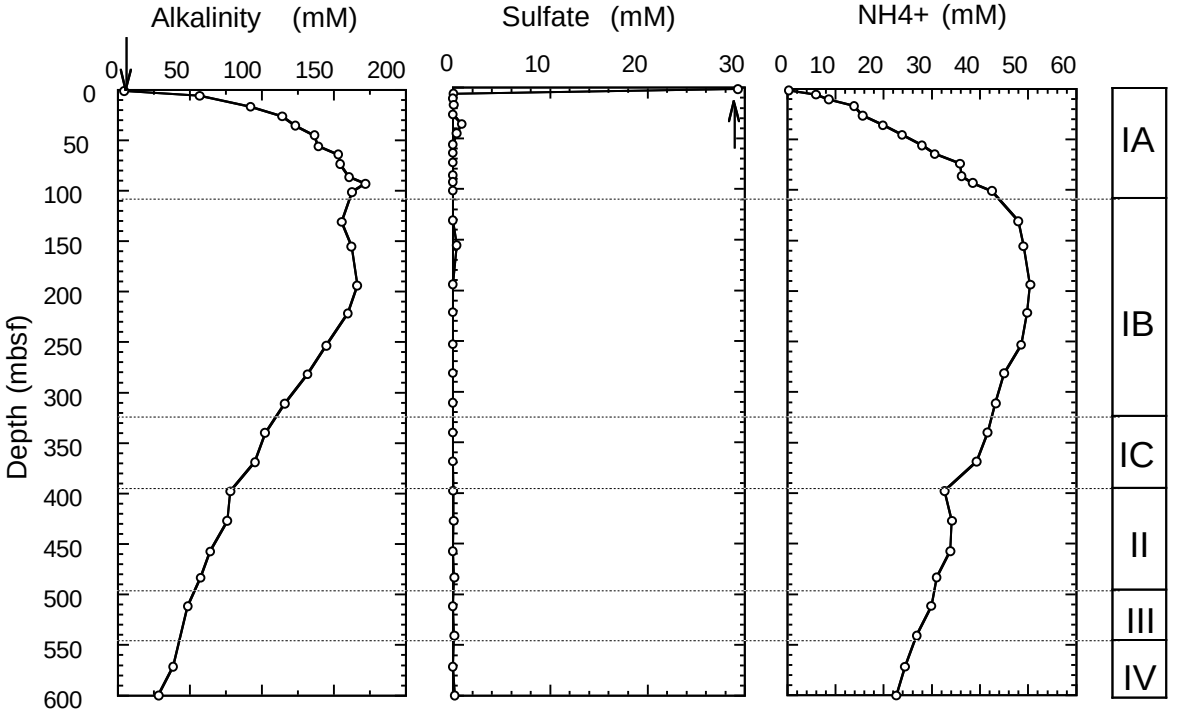
Alkalinity (mM)
Sulfate (mM)
NH4+ (mM)
Depth (mbsf)
0
50
100
150
200
250
300
350
400
450
500
550
600
0
10
20
30
40
50
60
IA
IB
IC
II
III
IV

Figure 8

OPERATIONS SYNOPSIS

The operations and engineering personnel aboard the *JOIDES Resolution* for Leg 175 were

Operations Manager:	Ron Grout
Schlumberger Engineer:	Steven Kittredge

TRANSIT FROM LAS PALMAS TO SITE 1075

The last line in Las Palmas cleared the dock at 2000 hr local time on 12 August 1997. The 3019-nmi sea voyage to proposed Site LCB-1 required 11 days at an average speed of 11.6 kt. The vessel speed was enhanced by favorable currents (Canary and the Equatorial Countercurrent) as well as calm environmental conditions. The *JOIDES Resolution* crossed the equator at 0° longitude at 0613 hr on 21 August. After a short seismic survey, a Datasonics 354M beacon was deployed at Site 1075 at 1950 hr on 21 August.

SITE 1075
(Proposed Site LCB-1)

Hole 1075A

Hole 1075A was spudded at 0450 hr on 24 August. The recovery of 1.50 m of sediment established the seafloor depth at 3007.0 m below rig floor (mbrf) by drill pipe measurement (DPM). APC Cores 175-1075A-1H through 22H were taken from 0 to 201.0 mbsf, with 201.0 m cored and 215.2 m recovered (106.3% recovery). Cores were oriented starting with 4H. The drill string was pulled back with the bit clearing the mudline at 2340 hr on 24 August, thereby ending Hole 1075A.

Hole 1075B

The vessel was offset 10 m to the east, and Hole 1075B was spudded at 0040 hr on 25 August. The first core indicated a water depth of 3006.5 mbrf by DPM. APC Cores 175-1075B-1H through 22H were taken from 0 to 204.5 mbsf, with 204.5 m cored and 215.0 m recovered (105.1% recovery). Cores were oriented starting with 4H. The drill string was pulled back with the bit clearing the mudline at 1810 hr on 25 August, ending Hole 1075B.

Hole 1075C

The vessel was offset another 10 m to the east where the third hole of the site was spudded with

the APC at 1855 hr on 25 August. The seafloor depth of Hole 1075C was determined at 3006.8 mbrf by DPM. After coring 22 hydraulic piston cores, the hole was terminated after reaching the depth objective of 207.2 m with an overall recovery of 103.0%. Cores were oriented starting with 3H. The bit cleared the seafloor at 1220 hr on 26 August. As the drill string was being pulled out of the hole, the beacon was released and recovered and the hydrophones and thrusters were retracted and secured.

SITE 1076
(Proposed Site LCB-4)

Hole 1076A

The 64-nmi voyage from Site 1075 to Site 1076 was accomplished at an average speed of 11.4 kt. As the vessel slowly approached the location using global positioning system (GPS) coordinates, the beacon was deployed at 2338 hr on 26 August. At 0440 hr on 27 August, the bit was positioned at 1411.0 mbrf, where Hole 1076A was spudded at 0440 hr on 27 August. The seafloor depth was established at 1415.7 mbrf DPM. APC Cores 175-1076-1H through 22H were taken from 0 to 204.3 mbsf, with 204.3 m cored and 217.5 m recovered (106.3% recovery). Cores were oriented starting with 3H. The Adara temperature tool heat-flow shoe was deployed at Cores 3H (23.8 mbsf), 5H (42.8 mbsf), 8H (71.3 mbsf), and 11H (99.8 mbsf). The calculated heat-flow gradient is 44.7˚C/km. Headspace analysis of the cores indicate the presence of biogenic methane with minute amounts of ethane (less than 28 ppm) and no discernable amounts of heavier hydrocarbons. The methane concentration peaked at 66 mbsf (69,000 ppm) and gradually tapered off with depth. Although some of the core exuded a mild sulphurous smell, any concentration of H_2S was below 1 ppm and could not be measured. The drill string was pulled back with the bit clearing the seafloor at 1830 hr on 27 August, ending Hole 1076A.

Hole 1076B

The vessel was offset 10 m to the east, and Hole 1076B was spudded at 1908 hr on 27 August. The seafloor depth was established at 1413.6 mbrf by DPM. After seven APC cores (0-60.9

mbsf), the hole was abandoned because no core was recovered in Cores 1076B-5H, 6H, and 7H. It was assumed that the bit had reentered the previous hole in the section after recovering Core 4H. The drill string was pulled out of the hole and cleared the seafloor at 2250 hr on 27 August, ending Hole 1076B.

Hole 1076C

The vessel was offset 20 m to the east, and Hole 1076C was spudded at 2325 hr on 27 August. APC Cores 1076C-1H through 22H were taken from 0 to 203.1 mbsf, with 203.1 m cored and 216.8 m recovered (106.8% recovery). Cores were oriented starting with 4H. The drill string was pulled out of the hole with the bit clearing the seafloor at 1155 hr on 28 August.

Hole 1076D

The vessel was offset another 20 m to the east where the fourth and final hole of the site was spudded with the APC at 1230 hr on 28 August. The seafloor depth was established at 1412.5 mbrf by DPM. APC Cores 1076D-1H through 12H were taken from 0 to 113.5 mbsf, with 113.5 m recovered (104.3%). The hole was aborted before the initial depth objective because of time constraints. The bit cleared the seafloor at 2030 hr on 28 August. While the drill string was being secured, the beacon was released and recovered at 2100 hr on 29 August, ending operations at Site 1076.

SITE 1077
(Proposed Site LCB-3A)

Hole 1077A

The 40-nmi voyage from Site 1076 to Site 1077 was accomplished at an average speed of 12.5 kt. As the vessel slowly approached the location using GPS coordinates, the beacon was deployed at 0534 hr on 29 August. Following an unsuccessful attempt at a mudline core from 2385.0 mbrf, the bit was positioned at 2387.0 mbrf where Hole 1077A was spudded at 1210 hr on 29 August. The seafloor depth was established at 2391.5 mbrf by DPM. APC Cores 175-1077A-1H through

22H were taken from 0 to 204.5 mbsf, with 204.5 m cored and 209.5 m recovered (102.2% recovery). Cores were oriented starting with 4H. The Adara temperature tool heat-flow shoe was deployed at Cores 5H (43.0 mbsf), 7H (62.0 mbsf), 10H (90.5 mbsf), and 13H (119.0 mbsf). The calculated heat-flow gradient is 56.8°C/km. Headspace analysis of the cores indicated the presence of biogenic methane with insignificant amounts of ethane (less than 10 ppm) and no discernable amounts of heavier hydrocarbons. The methane concentration peaked at 57 mbsf (54,717 ppm) and gradually tapered off with depth with another peak at 152 mbsf (44,860 ppm). While some of the core exuded a mild sulfurous smell, any concentration of H_2S was below 1 ppm and could not be measured.

Logging in Hole 1077A

Hole 1077A was logged with a limited suite of sensors to identify and locate the presence of gas hydrate in the sediments and to provide data for core-log integration. After a "go-devil" was pumped down the pipe to ensure the proper operation of the lockable float valve, the drill pipe was tripped to 63.5 mbsf, the top drive was picked up, and the bit was placed at 79.0 mbsf. The logging tool included the spectral gamma ray (NGT), long-spacing sonic (LSS), phasor dual induction (DITE-SFR), and the TLT sondes and was deployed at 0725 hr on 30 August. The tool logged Hole 1077A at 400 m/hr from 202 to 79 mbsf. By 1115 hr on 30 August, the logging equipment was rigged down, and the top drive was set back as the drill string was pulled to the surface. The bit cleared the seafloor at 1130 hr on 30 August, ending operations at Hole 1077A.

Hole 1077B

The vessel was offset 20 m to the west, and Hole 1077B was spudded at 1235 hr on 30 August. The seafloor depth was established at 2392.9 mbrf by DPM. APC Cores 175-1077B-1H through 22H were taken from 0 to 205.1 mbsf, with 205.1 m cored and 212.7 m recovered (103.6% recovery). The drill string was pulled back with the bit clearing the seafloor at 0455 hr on 31 August, ending operations at Hole 1077B.

Hole 1077C

The vessel was offset 20 m to the west, and Hole 1077C was spudded with the APC at 0550 hr on

31 August. The seafloor depth was estimated from recovery to be at 2396.7 mbrf. Three APC cores were taken to a depth of 22.8 mbsf when on-site operating time expired. Core recovery was only 72.2% of the cored interval because of the loss of watery sediments during the core retrieval process. The drill string was pulled out of the hole and cleared the seafloor at 0720 hr on 31 August, ending operations at Site 1077. By 1206 hr on 31 August, the drilling equipment was secured and the vessel was underway to Lobito, Angola, for a scheduled arrival at 0700 hr on 2 September to take the Angolan scientific observers on board.

SITE 1078
(Proposed Site MAB-1)

Hole 1078A

The vessel proceeded directly to the GPS coordinates of Site 1078 where a beacon was deployed at 2105 hr on 2 September. The bit was positioned at 436.5 m where Hole 1078A was spudded at 0040 hr on 3 September. The seafloor depth was established at 438.5 mbrf by DPM. APC Cores 175-1078A-1H through 8H were taken from 0 to 77.1 mbsf, which was considered APC refusal (recovery 100.4%). During the firing of Core 8H, a lock pin failed and left part of the sinker bar assembly and the core barrel at the bottom of the drill string. It required three wireline fishing attempts to recover the sinker bar hardware and another wireline trip to recover the full core barrel. The Adara temperature tool heat-flow shoe was deployed with Cores 3H (26.5 mbsf) and 6H (55.0 mbsf). An XCB core (9X) advanced the hole to 77.1 mbsf with 20% recovery. This was considered the total depth of the hole. The drill string was pulled back with the bit clearing the seafloor at 0800 hr on 3 September, ending Hole 1078A.

Hole 1078B

The vessel was offset 30 m to the south, and Hole 1078B was spudded at 0837 hr on 3 September. The seafloor depth was established at 437.4 mbrf by DPM. APC Cores 1078B-1H through 14H were taken from 0 to 130.1 mbsf, with 130.1 m cored and 125.7 m recovered (96.6% recovery). Cores were oriented starting with 3H. The Adara temperature tool heat-flow

shoe was deployed with 11H (101.6 mbsf) and 14H (130.1 mbsf). The drill string was pulled out of the hole and cleared the seafloor at 1810 hr on 3 September, ending Hole 1078B.

Hole 1078C

The vessel was offset 30 m to the south, and Hole 1078C was spudded at 1905 hr on 3 September. The seafloor depth was established at 437.3 mbrf by DPM. APC Cores 1078B-1H through 14H were taken from 0 to 130.1 mbsf and deepened, with the XCB to 165.2 m with 165.2 m cored and 149.6 m recovered (90.5% recovery). Cores were oriented starting with 3H. The drill string was pulled out of the hole and cleared the seafloor at 0535 hr on 4 September, ending Hole 1078C.

Hole 1078D

One more time, the vessel was offset 30 m to the south, and Hole 1078D was spudded at 0605 hr on 4 September. The seafloor depth was established at 438.7 mbrf by DPM. APC Cores 1078B-1H through 14H were taken from 0 to 126.8 mbsf, with 126.8 m cored and 116.7 m recovered (92.1% recovery). Cores were not oriented. The drill string was pulled out of the hole and cleared the seafloor at 1300 hr on 4 September, ending operations at Site 1078.

SITE 1079
(Proposed Site MAB-2)

Hole 1079A

The vessel proceeded in dynamic positioning (DP) mode to the GPS coordinates of Site 1079, where a beacon was deployed at 1604 hr on 4 September. A second beacon was dropped at 1650 hr as a precautionary measure because of erratic acoustics initially attributed to a distorted beacon signal. It was later determined that fishing boats in the area were transmitting signals that temporally affected the DP system and the precision depth recorder (PDR). Hole 1079A was spudded at 2007 hr on 4 September. The seafloor depth was established at 749.2 mbrf by DPM. APC Cores 175-1079A-1H through 14H were taken from 0 to 121.0 mbsf, with 121.0 m cored

and 124.6 m recovered (103.0%). Cores were oriented starting with 4H. No Adara temperature tool heat-flow measurements were taken at this site. The drill string was pulled out of the hole with the top drive, and the bit cleared the seafloor at 0355 hr on 5 September, thereby ending Hole 1079A.

Hole 1079B

The vessel was offset 30 m to the south, and Hole 1079B was spudded with the APC at 0430 hr on 5 September. The seafloor depth was established at 749.5 mbrf by DPM. APC Cores 1079B-1H through 14H were taken from 0 to 128.3 mbsf, with 128.3 m cored and 129.7 m recovered (101.1% recovery). Cores were oriented starting with 3H. The drill string was pulled out of the hole and cleared the seafloor at 1155 hr on 5 September, ending Hole 1079B.

Hole 1079C

The vessel was offset 30 m to the south, and Hole 1079C was spudded with the APC at 1225 hr on 5 September. The seafloor depth was established at 749.2 mbrf by DPM. APC Cores 1079C-1H through 14H were taken from 0 to 126.8 mbsf, with 126.8 m cored and 129.9 m recovered (102.4% recovery). Cores were oriented starting with 4H. The drill string was pulled out of the hole and cleared the seafloor at 2035 hr on 5 September, ending operations at Site 1079.

SITE 1080
(Proposed Site SAB-2)

Hole 1080A

After a 314-nmi voyage at an average speed of 10.7 kt, the vessel proceeded directly to the GPS coordinates of the site, where a beacon was deployed at 0407 hr on 7 September. Hole 1080A was spudded at 1020 hr on 7 September. The seafloor depth was established at 2777.2 mbrf by DPM. APC coring advanced to 50.8 mbsf, which was considered APC refusal, when an attempt at the seventh piston core resulted in no advance because of contact with a very hard layer. Cores were oriented starting with 4H. The hole was then deepened with the XCB from 50.8 to 52.1 mbsf with

high torque and very little penetration. After 20 min of rotation, the core barrel was recovered containing 0.12 m of dolomite, and the hole was terminated. The bit cleared the seafloor at 1730 hr on 7 September.

Hole 1080B

The vessel was offset 40 m to the south, and Hole 1080B was spudded with the APC at 1845 hr. APC coring advanced to 37.7 mbsf. When the attempt at Core 1080B-5H resulted in no advance of the core barrel because of a hard sediment layer, an XCB core barrel was dropped (5X) and advanced 0.5 m in 25 min of rotation. The decision was made to terminate the site, and the drill string was pulled back to 2767.0 m, clearing the seafloor at 0025 hr on 8 September. The hydrophones and thrusters were retracted and the drilling equipment was secured for transit by 0600 hr, thereby ending operations at Site 1080.

SITE 1081
(Proposed Site WR-1A)

Hole 1081A

The 184-nmi voyage to Site 1081 was impeded by rough seas and the northward flowing Benguela Current. The vessel steered into 1.5-m swells generating up to 5˚ of pitch angle, which combined with the countercurrent, slowed the forward progress to 8 kt. By the time the *JOIDES Resolution* reached Site 1081, the seas had flattened out and the average speed had increased to 9.4 kt. The vessel proceeded directly to the GPS coordinates of the site and deployed a beacon at 0200 hr on 9 September. Hole 1081A was spudded with the APC at 0530 hr on 9 September. The seafloor depth was established at 805.5 mbrf by DPM. APC coring advanced without incident to 134.0 mbsf (Cores 1081A-1H through 15H). Core 1081A-16H advanced only 3 m, and coring operations were switched to the XCB system. The XCB penetrated through a 1-m-thick firm horizon and then quickly advanced into softer sediments. Operations were switched back to piston coring. Core 1081A-18H advanced the hole to 154.5 mbsf using advancement by recovery. Core 1081A-19H failed to advance because of stiffer sediments, and XCB coring was again initiated.

The total penetration with the APC was 145.5 m with 103.9% recovery. Cores were oriented starting with 4H. Adara temperature tool heat-flow measurements were taken at 29.5 mbsf (4H), 58.0 mbsf (7H), 86.5 mbsf (10H), 115.0 mbsf (13H), and 137.0 mbsf (16H). XCB coring advanced to 452.7 mbsf (49X), which was the revised depth objective at Site 1081. The penetration with the XCB was 307.2 m with 78.9% recovery. The total recovery of Hole 1081A was 86.9%.

Logging Operations in Hole 1081A

In preparation for logging, an aluminum go-devil was dropped to ensure the opening of the lockable float valve. After the hole was flushed with a high-viscosity mud, the drill string was pulled back to 403.7 mbsf, where the top drive was set back. The drill bit was then placed at the logging depth of 101.2 mbsf. Hole 1081A was logged with a full suite of sensors to continuously characterize the sedimentary changes as a proxy for the paleoclimatic record and to provide data for core-log integration. For each run, the pipe was set at 101 mbsf and pulled back to 71 mbsf during logging. The wireline logging heave compensator was started when the logging tools reached the mudline. Logging operations began at 0200 hr on 9 September. The first log was conducted with the seismic-stratigraphic suite (25.8 m long). This suite was made up of the NGT, LSS, DITE-SFR, and TLT sondes. This tool string was deployed in the pipe at 0245 hr and logged the hole up from 450.5 mbsf. The tool was recovered at 0550 hr. The second log was with the lithoporosity suite (19.5 m long) and included the hostile-environment gamma spectrometry (HNGS), accelerator porosity (APS), lithodensity (LDS), and TLT sondes. The tool was deployed at 0655 hr and logged the hole from 450.5 to 71 mbsf. The third log was made with the Formation MicroScanner (FMS) suite (12.10 m long) and included the NGT, general purpose inclinometer (GPIT), and FMS sondes. This tool logged the hole from 450.5 mbsf. The tool was recovered at 1425 hr. The fourth and last log was with the magnetic susceptibility suite (11.8 m long) and included the NGT, magnetic susceptibility (SUMT), and the nuclear resonance magnetometer (NRMT) sondes. The tool was deployed in the pipe at 1455 hr and logged the hole from 450.5 to 71 mbsf. It was retrieved at 1740 hr. The logging equipment was rigged down by 1830 hr on 9 September. The hole was filled with heavy mud. The drill string was then pulled out of the hole, with the bit clearing the seafloor at 2115 hr on 11 September, ending operations at Hole 1081A.

Hole 1081B

The vessel was offset 30 m to the south, and Hole 1081B was spudded with the APC at 2220 hr on 11 September. The seafloor depth was established at 804.5 mbrf by DPM. APC coring advanced without incident to refusal at 187.6 mbsf with 104.4% recovery. Cores were oriented starting with 4H. The bit cleared the seafloor at 0925 hr on 12 September, thereby ending operations at Hole 1081B.

Hole 1081C

The vessel was offset 30 m to the south, and Hole 1081C was spudded with the APC at 0955 hr. The seafloor depth was established at 805.2 mbrf by DPM. APC coring advanced routinely to refusal at 155.2 mbsf. The recovery was 103.7%. Cores were oriented starting with 1081C-3H. The bit cleared the seafloor at 1815 hr, thereby ending operations at Site 1081.

SITE 1082
(Proposed Site WB-B)

Hole 1082A

The 93-nmi voyage to Site 1082 was accomplished at an average speed of 11.6 kt. The vessel approached the GPS coordinates of the site and deployed a beacon at 0445 hr on 13 September. Hole 1082A was spudded with the APC at 0750 hr. The seafloor depth was established from the recovery of the first core at 1290.7 mbrf. APC coring advanced without incident to 128.6 mbsf with 104.9% recovery. Cores were oriented starting with 3H. Adara temperature tool heat-flow measurements were taken at 45.8 (5H), 64.8 (7H), 83.8 (9H), and 102.8 mbsf (11H). The hole was deepened with the XCB to 600.6 mbsf (64X), which was the depth objective for this site. The penetration with the XCB was 472.0 m with 77.8% recovery.

Logging Operations in Hole 1082A

In preparation for logging, an aluminum go-devil was dropped to ensure the opening of the

lockable float valve, and the hole was flushed with a high-viscosity mud treatment. The drill string was then pulled up, and the bit was placed at the logging depth of 94.1 mbsf. Hole 1082A was logged with a full suite of sensors. For each run, the pipe was set at 94.1 mbsf and pulled back to 65.0 mbsf during logging. Logging operations began at 0200 hr on 15 September. The first log was conducted with the seismic-stratigraphic suite (25.8 m long). This suite was made up of the NGT, LSS, DITE-SFR, and TLT sondes. This tool string was deployed in the pipe at 0255 hr and logged the hole up from 599.3 mbsf. The tool was recovered at 0700 hr. The second log was made with the lithoporosity suite (19.5 m long) and included the HNGS, APS, LDS, and TLT sondes. The tool was deployed at 0800 hr and logged the hole up from bottom at 599.3 mbsf. The tool was pulled out of the pipe at 1225 hr. The third logging run was made with the FMS suite (12.10 m long) and included the NGT, GPIT, and FMS sondes. This tool was deployed at 1325 hr and logged the hole from 599.3 mbsf. The tool was recovered at 1700 hr. The fourth and last log was with the magnetic susceptibility suite (11.8 m long) and included the NGT, SUMT, and NRMT sondes. The tool was deployed in the pipe at 1730 hr and logged the hole from 599.3 mbsf. It was retrieved at 2010 hr. The logging equipment was rigged down by 2100 hr, and the hole was filled with heavy mud. The drill string was then pulled out of the hole, with the bit clearing the seafloor at 0005 hr on 16 September.

Hole 1082B

The vessel was offset 30 m to the south, and Hole 1082B was spudded with the APC at 0110 hr on 16 September. The recovery of the first core established the seafloor depth at 1291.8 mbrf. APC coring advanced without incident to refusal at 127.0 mbsf with 104.9% recovery. Cores were oriented starting with 4H. The bit cleared the seafloor at 0855 hr on 16 September, thereby ending operations at Hole 1082B.

Hole 1082C

Hole 1082C was spudded with the APC at 0855 hr on 16 September. The recovery of the first core established the seafloor depth at 1293.5 m. APC coring advanced to 202.0 mbsf with 107.8% recovery. The last two cores (Cores 175-1082C-23H and 24H) were partial strokes. Cores were oriented starting with 3H. The drill string was then retrieved, with the bit clearing the seafloor at

2315 hr. The beacon was recovered, and the hydrophones and thrusters were retracted. At 0200 hr on 17 September, the vessel was under way to Site 1083.

SITE 1083
(Proposed Site WB-C)

Hole 1083A

The 55-nmi voyage to Site 1083 was accomplished at an average speed of 12.5 kt. The vessel approached the GPS coordinates of the site and deployed a beacon at 0510 hr on 17 September. Hole 1083A was spudded with the APC at 1000 hr. The seafloor depth was established from the recovery of the first core at 2189.7 m. APC coring advanced without incident to 201.3 mbsf with 92.1% recovery. APC refusal was reached when the core barrel of Core 1083A-22H got stuck and required drilling over. Cores were oriented starting with 3H. The bit cleared the seafloor at 0225 hr on 18 September, thereby ending operations at Hole 1083A.

Hole 1083B

The vessel was offset 30 m to the south, and Hole 1083B was spudded with the APC at 0405 hr. The recovery of the first core established the seafloor depth at 1294.7 m. APC coring advanced to 202.3 mbsf with 102.0% recovery. The last core (Core 175-1083B-22H) required redrilling to free the stuck core barrel. Cores were oriented starting with 4H. The bit cleared the seafloor at 2110 hr on 18 September.

Holes 1083C and 1083D

The vessel was offset 30 m to the south. Hole 1083C consists of one failed mudline core. Hole 1083D was spudded with the APC at 2350 hr on 18 September. The recovery of the first core established the seafloor depth at 2189.9 m. APC coring advanced to 196.1 mbsf with 103.0% recovery. Cores were oriented starting with 3H. The drill string was retrieved, with the bit clearing the seafloor at 1420 hr and the plane of the rotary table at 1855 hr on 19 September. The beacon was recovered, and the hydrophones and thrusters retracted. The vessel was under way to Site

1084 were at 1900 hr on 19 September.

SITE 1084
(Proposed Site NCB-2B)

Hole 1084A

The 294-nmi voyage to Site 1084 was accomplished at an average speed of 9.3 kt. The vessel approached the GPS coordinates of the site and deployed a beacon at 0310 hr on 21 September. Hole 1084A was spudded with the APC at 0810 hr. The seafloor depth was estimated from the recovery of the first core at 2003.5 m. APC coring advanced without incident to 149.5 mbsf (Cores 1084A-1H through 17H), which was considered refusal depth for piston coring. Core recovery for the APC in Hole 1084A was 104.9%. Cores were oriented starting with 4H. Adara temperature tool heat-flow measurements were taken at 60.0 (7H), 79.0 (9H), 117.0 (13H), and 136.0 mbsf (15H). Hole 1084A was extended with the XCB to 605.0 mbsf (65X), which was the depth objective for this site. The penetration with the XCB was 455.5 m with 77.9% recovery. The total recovery of Hole 1084A was 84.6% of the cored interval.

Logging Operations in Hole 1084A

In preparation for logging, an aluminum go-devil was dropped to ensure the opening of the lockable float valve. After the hole was flushed with a high-viscosity mud treatment, the drill string was pulled back to 565.5 mbsf, where the top drive was set back. The drill string was then placed at the logging depth of 89.7 mbsf.

Hole 1084A was logged with a full suite of sensors. For each run, the pipe was set at 89.7 mbsf and pulled back to 59.0 mbsf during logging. The wireline logging heave compensator was started when the logging tools reached the mudline. Logging operations began at 0715 hr on 23 September. The first log was conducted with the seismic-stratigraphic suite (25.8 m long). This suite was made up of the NGT, LSS, DITE-SFR, and TLT sondes. The tool string was deployed in the pipe at 0905 hr and logged the hole up from 601.0 mbsf. The tool was recovered at 1330 hr.

The second log was run with the lithoporosity suite (19.5 m long) and included the hostile HNGS, APS, LDS, and TLT sondes. The tool was deployed at 1425 hr and logged the hole from 601.0 mbsf. The tool was retrieved at 1900 hr. The third log was made with the FMS suite (12.10 m long) and included the NGT, GPIT, and FMS sondes. This tool was deployed at 2310 hr and logged the hole from 604.5 mbsf. The tool was recovered by 2245 hr. The fourth and last log was with the magnetic susceptibility suite (11.8 m long) and included the NGT, SUMT, and NRMT sondes. The tool was deployed in the pipe at 2310 hr and logged the hole from 603.6 mbsf. It was retrieved at 0210 hr on 24 September. The logging equipment was rigged down by 0300 hr. The drill string was then pulled out of the hole, with the bit clearing the seafloor at 0315 hr on 24 September.

Hole 1084B

The vessel was offset 30 m to the north and Hole 1084B was spudded with the APC at 0415 hr. The recovery of the first core established the seafloor depth at 2004.4 m. APC coring advanced without incident to refusal at 182.8 mbsf (Cores 175-1084B-1H through 20H) with 102.1% recovery. Cores were oriented starting with 4H. The bit cleared the seafloor at 1750 hr on 24 September, thereby ending operations at Hole 1084B.

Hole 1084C

The vessel was offset 30 m to the north, and Hole 1084C was spudded with the APC on 24 September. The recovery of the first core established the seafloor depth at 2002.0 m. APC coring advanced to 202.0 mbsf (Cores 175-1084C-1H through 22H) with 104.9% recovery. Cores were oriented starting with 3H. The drill string was retrieved, with the bit clearing the seafloor at 0835 hr and the plane of the rotary table at 1225 hr on 25 September, thereby ending operations at Site 1084.

SITE 1085
(Proposed Site MCB-2A)

Hole 1085A

The 237-nmi voyage to Site 1085 was accomplished at an average speed of 10.1 kt. The speed of the vessel was adversely affected because of the northward flowing Benguela Current, combined with rough seas. The vessel approached the GPS coordinates of the site and deployed a beacon at 1215 hr on 26 September. Hole 1085A was spudded with the APC at 1653 hr. The seafloor depth was estimated from the recovery of the first core at 1724.8 m. APC coring advanced without incident to 305.0 mbsf (Cores 175-1085A-1H through 33H) with 96.2% recovery, which was considered refusal depth for piston coring. Cores were oriented starting with 4H. Adara temperature tool heat-flow measurements were taken at 41.7 (5H), 60.7 (7H), 79.7 (11H), and 231.7 mbsf (25H). XCB coring advanced to 605.0 mbsf (64X) with 100.7% recovery.

Logging Operations in Hole 1085A

In preparation for logging, an aluminum go-devil was dropped to ensure the opening of the lockable float valve. After the hole was flushed with a high-viscosity mud treatment, the bit was placed at the logging depth of 88.3 mbsf. Hole 1085A was logged with a full suite of sensors. For each run, the pipe was set at 88.3 mbsf and pulled back to 60.0 mbsf during logging. The wireline logging heave compensator was started when the logging tools reached the mudline.

Logging operations began at 0030 hr on 29 September. The first log was conducted with the seismic-stratigraphic suite (25.8 m long). This suite was made up of the NGT, LSS, DITE-SFR, and TLT sondes. This tool string was deployed in the pipe at 0110 hr and logged the hole from 603.2 mbsf. The tool was recovered at 0510 hr. The second log was with the lithoporosity suite (19.5 m long) and included the HNGS, APS, LDS, and TLT sondes. The tool was deployed at 0620 hr and logged the hole up from 600.7 mbsf. The tool was retrieved at 1020 hr. The third log was made with the FMS suite (12.10 m long) and included the NGT, GPIT, and FMS sondes. This tool was deployed at 1125 hr and logged the hole from 600.7 mbsf. The tool was recovered by 1400 hr. The fourth and last log was with the magnetic susceptibility suite (11.8 m long) and

included the NGT, SUMT, and NRMT sondes. The tool was deployed in the pipe at 1425 hr and logged the hole from 600.7 mbsf. It was retrieved at 1715 hr on 29 September. The logging equipment was rigged down by 1800 hr. The drill string was then pulled out of the hole, with the bit clearing the seafloor at 1815 hr on 29 September, thereby ending operations at Hole 1085A.

Hole 1085B

The vessel was offset 30 m to the west, and Hole 1085B was spudded with the APC at 1915 hr. The recovery of the first core established the seafloor depth at 1724.6 m. APC coring advanced without incident to refusal at 321.2 mbsf (Cores 175-1085A-1H through 35H) with 101.7% recovery. The last two cores did not achieve full piston strokes due to the indurated sediments. Cores were oriented starting with 3H. The drill string was retrieved, and the bit cleared the seafloor at 1730 hr. After the beacon, hydrophones, and thrusters were retracted and the drilling equipment was secured, the vessel was under way to the next site at 2330 hr on 30 September.

Site 1086
(Proposed Site SCB-E)

Hole 1086A

The 157-nmi voyage to Site 1086 was accomplished at an average speed of 8.8 kt. The speed of the vessel was adversely affected because of the northward-flowing Benguela Current, combined with rough seas. The vessel approached the GPS coordinates of the site and deployed a beacon at 1900 hr on 1 October. Hole 1086A was spudded with the APC at 2240 hr. The seafloor depth was estimated from the recovery of the first core at 792.8 m. APC coring advanced without incident to 206.2 mbsf (Cores 175-1086-1H through 22H), which was considered refusal depth for piston coring. APC recovery for Hole 1086A was 102.4%. Cores were oriented starting with 3H. Adara temperature tool heat-flow measurements were not obtained at this site. The drill string was pulled out of the hole, with the bit clearing the seafloor at 0925 hr on 2 October, thereby ending Hole 1086A.

Hole 1086B

The vessel was offset 30 m to the west, and Hole 1086B was spudded with the APC at 1010 hr on 2 October. The recovery of the first core established the seafloor depth at 796.2 m. APC Cores 175-1086B-1H through 23H were taken from 0 to 212.1 mbsf with 101.7% recovery. The last core did not achieve a full piston stroke. Cores were oriented starting with 4H. The drill string was then retrieved, with the bit clearing the seafloor at 2230 hr. The beacon was recovered, and the hydrophones and thrusters were retracted. The vessel was under way to the next site at 0030 hr on 3 October.

SITE 1087A
(Proposed Site SCB-1)

Hole 1087A

The 19-nmi voyage to Site 1087 was accomplished at an average speed of 12.6 kt. The vessel approached the GPS coordinates of the site and deployed a beacon at 0210 hr on 3 October. Hole 1087A was spudded with the APC at 0600 hr and the seafloor depth was estimated from the recovery of the first core at 1383.3 mbrf. APC coring advanced without incident to 255.2 mbsf with 98.9% recovery, which was considered refusal depth for piston coring. Cores were oriented starting with Core 175-1087-3H. Adara temperature tool heat-flow measurements were taken at 46.2 (5H), 65.2 (7H), 93.7 (10H), and 122.2 mbsf (13H). The drill string was pulled out of the hole, with the bit clearing the seafloor at 2225 hr on 3 October, thereby ending operations at Hole 1087A.

Hole 1087B

The vessel was offset 30 m to the south, and Hole 1087B was spudded with the APC at 2317 hr. The recovery of the first core established the seafloor depth at 1383.5 mbrf. APC coring advanced without incident to 72.5 mbsf with 103.4% recovery. Cores were oriented starting with 3H. The bit was pulled out of the hole and cleared the seafloor at 0340 hr on 4 October, thereby ending Hole 1087B.

Hole 1087C

Hole 1087C was spudded with the APC at 0425 hr. The recovery of the first core established the seafloor depth at 1385.9 mbrf. Piston coring advanced to refusal at 248.6 mbsf. Cores were oriented starting with 4H. The hole was extended with the XCB to 491.9 mbsf with 91.8% recovery.

Logging Operations in Hole 1087C

In preparation for logging, an aluminum go-devil was dropped to ensure the opening of the lockable float valve. After the hole was flushed with a high-viscosity mud treatment, the drill string was pulled back to 442.8 mbsf, where the top drive was set back. The drill string was then placed at the logging depth of 85.8 mbsf. Logging operations began at 1930 hr on 5 October. The initial log was conducted with the seismic-stratigraphic suite (25.8 m long). This suite was made up of the NGT, LSS, DITE-SFR, and TLT sondes. This tool string was deployed in the pipe at 2015 hr and logged the hole down to and than up from 487.1 mbsf.

While attempting to recover the logging tool, the instrument hung up approximately 5 m inside the bit. Maximum overpull on the logging line was 1200 lbs. The logging tool was eventually freed from the bit by pumping. The logging winch operator tried to work the tool into the drill string again by incrementally pulling on the logging line up to a maximum of 4000 lbs head tension. This time the tool string became totally stuck in the bit and was unable to be worked up or down. Attempts at retrieving the logging tool with the logging cable were given up, and the Kinley cutter and crimper tools were prepared. The Kinley crimper was dropped, followed by a Kinley hammer. The drill string was pulled out of the hole, with the bit clearing the plane of the rotary table at 0715 hr. The logging tool was not recovered.

Hole 1087D

The vessel was offset 30 m to the south, and Hole 1087D was spudded at 1030 hr on 6 October. After drilling to 72.5 mbsf, piston coring was initiated. APC coring proceeded to 177.0 mbsf, which required the use of the last full-sized liner. A sole XCB core was then taken from 177.0 to

186.6 mbsf and recovered 9.88 m (102.9%). This core used the last liner on the vessel. The hole was then completed to a depth of 201.3 mbsf with two piston cores that were obtained without liners and recovered 100%. The total piston cored interval was 119.2 mbsf with 121.04 m (101.5%) recovered. The last core gave a total recovery for the leg of 8003.23 m. The drill string was then pulled out of the hole, with the bit clearing the seafloor at 2140 hr. The beacon was recovered at 2215 hr. The bit was at the rotary table at 0145 hr on 7 October. At 0700 hr on 7 October, the vessel departed the last site of Leg 175.

OCEAN DRILLING PROGRAM
OPERATIONS RESUME
LEG 175

Total Days (9 August 1997 to 8 October 1997)	**59.78**
Total Days in Port	**3.61**
Total Days Underway	**20.26**
Total Days on Site	**35.88**

	days
Drilling	**0.05**
Other	**0.52**
Tripping Time	**6.34**
Stuck pipe/Hole Trouble	**0.00**
Logging/Downhole Science	**4.00**
Mechanical Repair Time (Contractor)	**0.00**
Reentry Time	**0.00**
W.O.W.	**0.00**
Coring	**24.72**

Total Distance Traveled (nautical miles)	**5160.0**
Average Speed Transit (knots):	**10.9**
Number of Sites	**13.0**
Number of Holes	**40.0**
Number of Cores Attempted	**894.0**
Total Interval Cored (m)	**8210.5**
Total Core Recovery (m)	**8003.2**
% Core Recovery	**97.48**
Total Interval Drilled (m)	**72.5**
Total Penetration	**8283.0**
Maximum Penetration (m)	**605.0**
Minimum Penetration (m)	**9.5**
Maximum Water Depth (m from drilling datum)	**3007.0**
Minimum Water Depth (m from drilling datum)	**437.3**

LEG 175
TOTAL TIME DISTRIBUTION

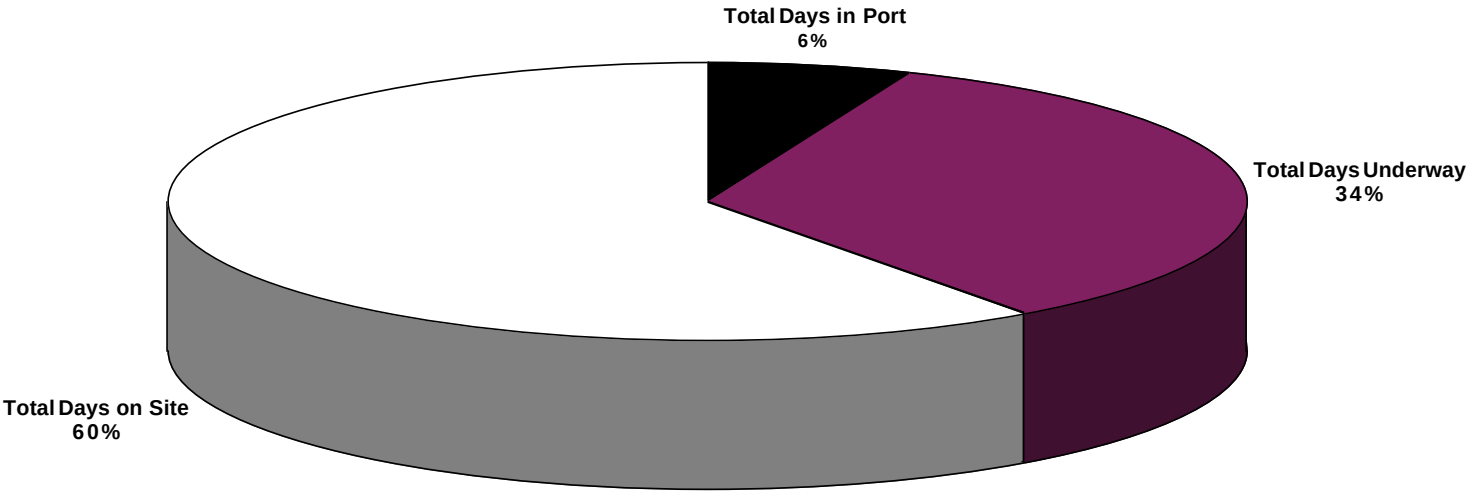

Total Days of Leg = 59.8

TECHNICAL REPORT

The ODP technical and logistics personnel aboard the *JOIDES Resolution* for Leg 175 were

Tim Bronk	Marine Lab Specialist: Chemistry
Roy Davis	Marine Lab Specialist: Photographer
Mike Hodge	Marine Computer Specialist
David Kotz	Marine Computer Specialist
Kuro Kuroki	Assistant Lab Officer
Jaque Ledbetter	Marine Lab Specialist: X-ray
Erinn McCarty	Marine Lab Specialist: Curator
Bill Mills	Lab Officer
Erik Moortgat	Marine Lab Specialist: Physical Properties
Chris Nugent	Marine Lab Specialist: Downhole Tools
Matt O'Regan	Marine Lab Specialist
Larry Obee	Marine Logistics Coordinator
Anne Pimmel	Marine Lab Specialist: Chemistry
Steve Prinz	Marine Lab Specialist: Curator
Jo Ribbens	Marine Lab Specialist: Yeoman
Peter Solheid	Marine Lab Specialist: Paleomagnetics
Bill Stevens	Marine Electronics Specialist
Mark Watson	Marine Electronics Specialist

OCEAN DRILLING PROGRAM
SITE SUMMARY
LEG 175

HOLE	LATITUDE	LONGITUDE	WATER DEPTH (mbrf)	NUMBER OF CORES	INTERVAL CORED (meters)	CORE RECOVERED (meters)	PERCENT RECOVERED (percent)	DRILLED (meters)	TOTAL PENETRATION (meters)	TIME ON HOLE (hours)	TIME ON SITE (days)
1075A	4°47.1198'S	10°4.4989'E	3007.0	22	201.00	213.75	106.3%	0.0	201.00	27.83	1.2
1075B	4°47.1197'S	10°4.5025'E	3006.5	22	204.50	215.03	105.1%	0.0	204.50	18.50	0.8
1075C	4°47.1206'S	10°4.5100'E	3006.8	22	207.20	213.47	103.0%	0.0	207.20	23.83	1.0
		1075 SITE TOTALS:		**66**	**612.70**	**642.25**	**104.8%**	**0.0**	**612.70**	**70.17**	**2.9**
1076A	5°4.1316'S	11°6.0917'E	1415.7	22	204.30	217.47	106.4%	0.0	204.30	18.75	0.8
1076B	5°4.1344'S	11°6.0922'E	1413.6	7	60.90	25.87	42.5%	0.0	60.90	4.42	0.2
1076C	5°4.1309'S	11°6.1048'E	1413.9	22	203.10	216.80	106.7%	0.0	203.10	13.00	0.5
1076D	5°4.1312'S	11°6.1150'E	1412.5	12	113.50	118.41	104.3%	0.0	113.50	14.33	0.6
		1076 SITE TOTALS:		**63**	**581.80**	**578.55**	**99.4%**	**0.0**	**581.80**	**50.50**	**2.1**
1077A	5°10.7969'S	10°26.1960'E	2391.5	22	204.50	208.99	102.2%	0.0	204.50	30.00	1.3
1077B	5°10.7977'S	10°26.1831'E	2392.9	22	205.10	211.53	103.1%	0.0	205.10	17.42	0.7
1077C	5°10.7995'S	10°26.1687'E	2396.7	3	22.80	16.46	72.2%	0.0	22.80	7.18	0.3
		1077 SITE TOTALS:		**47**	**432.40**	**436.98**	**101.1%**	**0.0**	**432.40**	**54.60**	**2.3**
1078A	11°55.2145'S	13°24.0134'E	438.5	9	77.10	70.28	91.2%	0.0	77.10	10.92	0.5
1078B	11°55.2318'S	13°24.0172'E	437.4	14	130.10	125.80	96.7%	0.0	130.10	10.17	0.4
1078C	11°55.2474'S	13°24.0161'E	437.3	18	165.20	149.58	90.5%	0.0	165.20	11.42	0.5
1078D	11°55.2661'S	13°24.0165'E	438.7	14	126.80	116.71	92.0%	0.0	126.80	8.92	0.4
		1078 SITE TOTALS:		**55**	**499.20**	**462.37**	**92.6%**	**0.0**	**499.20**	**41.42**	**1.7**
1079A	11°55.7785'S	13°18.5433'E	749.2	14	121.00	124.61	103.0%	0.0	121.00	11.85	0.5
1079B	11°55.7676'S	13°18.5393'E	749.5	14	128.30	129.70	101.1%	0.0	128.30	8.00	0.3
1079C	11°55.7969'S	13°18.5607'E	749.2	14	126.80	129.90	102.4%	0.0	126.80	10.58	0.4
		1079 SITE TOTALS:		**42**	**376.10**	**384.21**	**102.2%**	**0.0**	**376.10**	**30.43**	**1.3**
1080A	16°33.5803'S	10°49.2029'E	2777.2	7	52.10	55.57	106.7%	0.0	52.10	13.38	0.6
1080B	16°33.5963'S	10°49.2043'E	2779.3	5	38.20	40.06	104.9%	0.0	38.20	12.50	0.5
		1080 SITE TOTALS:		**12**	**90.30**	**95.63**	**105.9%**	**0.0**	**90.30**	**25.88**	**1.1**
1081A	19°37.1818'S	11°19.1598'E	805.5	49	452.70	393.48	86.9%	0.0	452.70	67.25	2.8
1081B	19°37.1981'S	11°19.1588'E	804.5	21	187.60	195.87	104.4%	0.0	187.60	12.17	0.5
1081C	19°37.2128'S	11°19.1620'E	805.2	17	155.20	160.94	103.7%	0.0	155.20	10.83	0.5
		1081 SITE TOTALS:		**87**	**795.50**	**750.29**	**94.3%**	**0.0**	**795.50**	**90.25**	**3.8**
1082A	21°5.6373'S	11°49.2361'E	1290.7	64	600.60	502.01	83.6%	0.0	600.60	67.25	2.8
1082B	21°5.6517'S	11°49.2326'E	1291.8	14	127.00	133.17	104.9%	0.0	127.00	8.42	0.4
1082C	21°5.6690'S	11°49.2342'E	1293.5	24	202.00	217.83	107.8%	0.0	202.00	17.58	0.7
		1082 SITE TOTALS:		**102**	**929.60**	**853.01**	**91.8%**	**0.0**	**929.60**	**93.25**	**3.9**
1083A	20°53.6841'S	11°13.0720'E	2189.7	22	201.30	185.32	92.1%	0.0	201.30	21.17	0.9
1083B	20°53.7004'S	11°13.0738'E	2194.7	22	202.30	206.41	102.0%	0.0	202.30	19.75	0.8
1083C	20°53.7138'S	11°13.0734'E	2190.5	1	9.50	9.78	102.9%	0.0	9.50	1.00	0.0
1083D	20°53.7138'S	11°13.0734'E	2189.9	21	196.10	201.94	103.0%	0.0	196.10	19.83	0.8
		1083 SITE TOTALS:		**66**	**609.20**	**603.45**	**99.1%**	**0.0**	**609.20**	**61.75**	**2.6**
1084A	25°30.8345'S	13°1.6668'E	2003.5	65	605.00	511.56	84.6%	0.0	605.00	72.08	3.0
1084B	25°30.8206'S	13°1.6665'E	2004.4	20	182.80	186.60	102.1%	0.0	182.80	14.58	0.6
1084C	25°30.8037'S	13°1.6670'E	2003.4	22	207.60	217.82	104.9%	0.0	207.60	18.67	0.8
		1084 SITE TOTALS:		**107**	**995.40**	**915.98**	**92.0%**	**0.0**	**995.40**	**105.33**	**4.4**
1085A	29°22.4665'S	13°59.4064'E	1724.8	64	604.00	594.39	98.4%	0.0	604.00	78.00	3.3
1085B	29°22.4657'S	13°59.3898'E	1724.6	35	321.20	326.51	101.7%	0.0	321.20	29.25	1.2
		1085 SITE TOTALS:		**99**	**925.20**	**920.90**	**99.5%**	**0.0**	**925.20**	**107.25**	**4.5**
1086A	31°33.1608'S	15°39.6235'E	792.8	22	206.20	211.09	102.4%	0.0	206.20	14.42	0.6
1086B	31°33.1588'S	15°39.6047'E	796.2	23	208.50	212.09	101.7%	0.0	208.50	15.08	0.6
		1086 SITE TOTALS:		**45**	**414.70**	**423.18**	**102.0%**	**0.0**	**414.70**	**29.50**	**1.2**
1087A	31°27.8813'S	15°18.6541'E	1383.3	27	255.20	252.38	98.9%	0.0	255.20	20.25	0.8
1087B	31°27.8975'S	15°18.6541'E	1383.5	8	72.50	74.83	103.2%	0.0	72.50	5.25	0.2
1087C	31°27.9137'S	15°18.6541'E	1385.9	53	491.90	478.30	97.2%	0.0	491.90	51.42	2.1
1087D	31°27.9299'S	15°18.6541'E	1383.5	15	128.80	130.92	101.6%	72.5	201.30	23.92	1.0
		1087 SITE TOTALS:		**103**	**948.40**	**936.43**	**98.7%**	**72.5**	**1020.90**	**100.83**	**4.2**
		LEG 175 TOTALS:		**894**	**8210.50**	**8003.23**	**97.5%**	**72.50**	**8283.00**	**861.17**	**35.9**

GENERAL LEG INFORMATION

The *D/V Joides Resolution* docked in Las Palmas, Canary Islands, on 9 August 1997, ending Leg 174B. On the following morning, the Leg 175 crew arrived and began crossover activities. On 12 August we were under way to our first site with a crew of 111. On 2 September we spent nine hours in Lobito, Angola, to pick up the Angolan observer, David Pato. While in port, the vessel was visited by Angolan government officials, students, and the local press. Drilling operations were completed by 7 October. After a one-day transit, the *D/V JOIDES Resolution* arrived in Cape Town, South Africa, on 8 October, ending Leg 175 operations. The participants of Leg 175 cored and analyzed a record-setting 8003.23 m of core from 13 sites (40 holes).

PORT CALL ACTIVITIES OVERVIEW

Logistic activities began as soon as the *D/V JOIDES Resolution* cleared Spanish Customs in Las Palmas. Most of the science and drilling supplies had been loaded during the previous port call in New York City, thus reducing the amount of work necessary to get the ship ready.

LAB ACTIVITIES

In addition to the standard sedimentological and paleontological analyses, high priority was given to the collection of core-core and core-log correlation data provided by the multisensor track, Minolta spectrophotometer, and cryogenic magnetometer.

Leg 175 severely tested our staff, facilities, and equipment. Many "manual" core-processing tasks could be automated to relieve some of the workload. Handling hazardous core materials was a problem that we dealt with during the leg. Most of the sites had either high H_2S levels (200+ ppm) or produced noxious organic gases.

TRANSIT ACTIVITIES

Navigational data were collected on all transits using standard GPS. Differential GPS was not available for the leg. Bathymetric and magnetic data were collected only on the transit from Las Palmas to our first site.

A seismic survey was used to locate our first site, but the remaining sites were located using GPS coordinates only. Both the multichannel and single-channel streamers were used during the seismic survey, but because of technical difficulties, we were unable to process the multichannel data. These data will be returned to shore for further processing.

LAB/SERVICE ACTIVITIES

Chemistry Lab

Interstitial water (IW) analyses included refractometric analysis for salinity; titration for pH, alkalinity, and chloride; ion chromatography for sulfate, potassium, sodium, calcium, and magnesium; and colorimetric analyses for silica, phosphate, and ammonium. Atomic absorption spectrophotometry was used to quantify concentrations of Sr in pore waters. High H_2S concentration in the pore waters required additional sample preparation before silica and phosphate analyses.

High-resolution IW sampling was performed on four out of 13 sites. It consisted of one IW per section for the first 60 m, then one per core until 100 m, and one every three cores thereafter. Around 350 analyses were done, leading to a heavy usage of the Dionex, AA, Cl titrator, and spectrophotometer.

Solid core samples were analyzed for inorganic and total carbon (using the coulometer and the carbon/nitrogen/sulfur analyzer [CNS]). Based on their organic carbon content, some samples

were selected and analyzed by the Rock-Eval. The system was used to determine S_1, S_2, and S_3. Gas chromatograph #3 and the natural gas analyzer were used to provide real-time monitoring of the volatile hydrocarbons and H_2S.

Computer Service

High recovery and the resulting volume of data overwhelmed the capacity of the shipboard server's disk space, causing numerous problems throughout the leg. Problems with Macintosh systems surfaced almost daily, some requiring reinstallation of the operating system. The mail system was also very unreliable during this leg. Hardware problems on the VAX and software problems on the NetWare servers caused repeated losses of service. The Laroux virus was a frequent nuisance but never caused any serious problems.

Core Lab

With more than 8000 m of core passing through the lab during the leg, it was fortunate that everything ran smoothly and there were no complications that required any serious modifications to either procedures or instruments. H_2S levels were monitored with sensors on the catwalk and with hand-held units on the splitting room. Cores were degassed on the catwalk and again in the splitting room until safe H_2S levels were obtained.

Curation

Routine shipboard and investigator samples were taken from the first hole at all sites. Sampling frequency was quite high but was revised as the cruise continued to accumulate the tremendous amount of core recovered and to ease the workload at the sampling table.

Downhole Measurements Lab

In situ temperature measurements were made at all sites. The APC/Adara cutting shoe was used for these measurements with a 94% success rate.

Microscopes

No problems reported.

Paleomagnetics Lab

This leg saw heavy use of the cryogenic magnetometer. All of the cores were measured plus several hundred discrete samples. Fortunately, the magnetometer and the LabView software ran with few problems. All APC cores were oriented using the tensor tool.

Photography Lab

No problems to report.

Physical Properties Lab

The MST and color reflectometry measurements were critical to the leg. Fortunately, there was only one minor problem with the *P*-wave logger that was solved by using the back up unit. The single-channel thermal conductivity unit was used throughout the leg and was more than able to keep up with the core flow.

Underway Geophysics Lab and Fantail

The starboard magnetometer was reheaded and is now working properly. The hydraulic motor for the starboard hose-bundle handler was repaired with a seal supplied by Sedco and with assistance from their mechanic.

With the captain’s permission, the void space over the sonar dome was opened. Careful testing confirmed that our 12kHz transducer was bad, as well as the bulkhead connector installed in the cover plate. A new transducer and connector were ordered. During some upcoming port call, the sonar dome will have to be pulled to affect repairs.

X-ray Lab

In addition to the "standard" X-ray diffraction (XRD) bulk analyses, the sedimentologists requested clay separations for analysis by XRD and analysis of standard mixtures for quantitative XRD calculations. They also expressed an interest in X-ray fluorescence (XRF) analyses of sediments. None of these requests could be accommodated because of the anticipated high core

recovery. Initially, it was agreed that one bulk XRD sample per core would be analyzed, but even this sampling rate proved to be impossible to maintain. After 411 bulk XRD samples, the X-ray lab was closed. No routine XRD samples were taken after Site 1082.

Electronic Service

The lab equipment operated satisfactorily during the leg. Compared with previous legs, no major problems that were out of the ordinary occurred with the majority of the equipment. As always, the first two weeks were spent addressing minor problems that were discovered during start-up operations. A great deal of time was spent removing the TOTCO (drilling-rig instrument company) hardware from the derrick.

Software Developments and Upgrades

- The MST software was upgraded to LabVIEW 4.1, and the natural gamma-ray data collection routine was modified to truncate the "garbage channels" from the spectrum data. The data server connect routine was modified to look for the DATA1 server.

- VS software was upgraded to LabVIEW 4.1, and the data server connect routine was modified to look for the DATA1 server.

- The Long Core software for the cryogenic magnetometer was upgraded to include a routine that displays the collected data in four plot formats: (1) intensity vs. decay, (2) vector demagnetization, (3) As-Zijiderveld, and (4) equal area.

- The stand-alone weighing programs for the chemistry and X-ray labs' weighing stations were replaced with a new Windows 95 LabVIEW application. The application uses a new weighing algorithm and provides a high-frequency filter option. A version for the Mac OS will be provided in the future.

- New versions of the MAD, T-TOOL, and COULOMETER software were installed during this leg.

- A new version of Depth-O-Matic was developed to replace the slow JANUS depth utility. Unlike the JANUS depth utility, Depth-O-Matic will work with tabs, commas, or space-delimited file formats. Also, it will work with data files that have multiple title lines. Depth-O-Matic can work with single files or load and concatenate multiple files in nested directories. The depth-matching algorithm is more efficient than the routine used by the JANUS depth utility; for example, the JANUS depth utility will take 45 min to process a file of 24,000 data points, whereas Depth-O-Matic only takes 3 min.

- New Thermal Conductivity software (V3.20) for the TK04 Thermal Conductivity Meter was brought to the ship and installed. The new software allows for the contact resistance of the probes and for the loss of heat into the probe half space. The quality of results is improved (can differ on the order of 1%), and an empirical correction of the thermal conductivity values obtained with half-space measurements is no longer necessary, even on samples with low thermal conductivity. The user interface and the appearance of the measuring and evaluation program remain the same. The changes are mainly internal.

LEG 175 STATISTICS

Sites:	14
Holes:	40
Meters Drilled (m):	8210.5
Meters Cored (m):	8210.5
Meters Recovered (m):	8003.23
Number of General Samples:	15763
Whole-Core MST:	
GRAPE (sections)	5728
Natural Gamma Radiation (sections)	2504
P-Wave (sections)	3459
Magnetic Susceptibility (sections)	5728
Physical Properties Lab:	
PVS#1 Velocity (samples)	6
PVS#2 Velocity	143
PVS#3 Velocity	1379
Vane Shear	1373
Penetrometer	0
Resistivity	0
Moisture-Density	3074
Thermoconductivity	208
X-ray Lab:	
X-ray Fluorescence	0
X-ray Diffraction	412
Thin Section Lab:	
Thin Sections	0
Chemistry Lab:	
Carbonates	1097
Gas	535
Interstitial Water	314
Downhole Measurements:	
Adara Temperature Measurements	34
WSTP Water Samples	0
Underway Geophysics:	
Total Transit (nautical miles)	5160
Bathymetry	2861

Magnetics	2861
Seismic	17